

AD

USAALABS TECHNICAL REPORT 69-61

INSTABILITY OF SPHERICAL CAPS AND COMPLETE SPHERES

AD736346

By

Philippe Jacques Jean-Marie Lebouc

September 1971

EUSTIS DIRECTORATE
U. S. ARMY AIR MOBILITY RESEARCH AND DEVELOPMENT LABORATORY
FORT EUSTIS, VIRGINIA

CONTRACT DAAJ02-67-C-0031
STANFORD UNIVERSITY
STANFORD, CALIFORNIA

Approved for public release;
distribution unlimited.



Reproduced by
NATIONAL TECHNICAL
INFORMATION SERVICE
Springfield, Va 22151

D D C
REF ID: A65747
FEB 3 1972
RUGER B
B

7

21

Unclassified

Security Classification

DOCUMENT CONTROL DATA - R & D

(Security classification of title, body of abstract and indexing annotation must be entered when the overall report is classified)

1. ORIGINATING ACTIVITY (Corporate author) Stanford University Stanford, California	2a. REPORT SECURITY CLASSIFICATION Unclassified
	2b. GROUP

3. REPORT TITLE

INSTABILITY OF SPHERICAL CAPS AND COMPLETE SPHERES

4. DESCRIPTIVE NOTES (Type of report and inclusive dates)

5. AUTHOR(S) (First name, middle initial, last name)

Philippe Jacques Jean-Marie Lebouc

6. REPORT DATE

September 1971

7a. TOTAL NO. OF PAGES

78

7b. NO. OF REFS

25

8a. CONTRACT OR GRANT NO.

DAAJ02-67-C-0031

8b. PROJECT NO.

Task 1F162204A17002

c.

10. DISTRIBUTION STATEMENT

Approved for public release; distribution unlimited.

11. SUPPLEMENTARY NOTES

12. SPONSORING MILITARY ACTIVITY

Eustis Directorate, U. S. Army Air Mobility Research and Development Laboratory, Fort Eustis, Virginia

13. ABSTRACT

The general analysis of instability made by Westergaard (Ref. 1) in 1922 indicates that the deformation of a body, the initial imperfection, and the critical and actual load levels can be associated by a single law. Southwell (Ref. 2), in independent research made in 1932, examined this situation in detail for a column and proposed a method of plotting experimental results for imperfect specimens which could predict the instability load for the perfect column. He indicated in his paper that the process should have a wider content than that in which he worked. Subsequent research has verified this conjecture for a wide range of problems.

This report is concerned with the instability behavior of spherical shells for which, so far as can be traced from a broad literature survey, no application of this technique has been considered. Moreover, it is an area in which the scatter between experimental results is normally great and in which there is still considerable analytical effort being made.

The report demonstrates that the Southwell Plot approach gives an interpretation of experimental data which is consistent with the findings of small displacement computations.

DD FORM 1 NOV 68 1473

REPLACES DD FORM 1473, 1 JAN 64, WHICH IS
OBSOLETE FOR ARMY USE.

Unclassified

Security Classification

DISCLAIMERS

The findings in this report are not to be construed as an official Department of the Army position unless so designated by other authorized documents.

When Government drawings, specifications, or other data are used for any purpose other than in connection with a definitely related Government procurement operation, the United States Government thereby incurs no responsibility nor any obligation whatsoever; and the fact that the Government may have formulated, furnished, or in any way supplied the said drawings, specifications, or other data is not to be regarded by implication or otherwise as in any manner licensing the holder or any other person or corporation, or conveying any rights or permission, to manufacture, use, or sell any patented invention that may in any way be related thereto.

Trade names cited in this report do not constitute an official endorsement or approval of the use of such commercial hardware or software.

DISPOSITION INSTRUCTIONS

Destroy this report when no longer needed. Do not return it to the originator.

COSTS		WHITE SECTION <input checked="" type="checkbox"/>
MFG		BUFF SECTION <input type="checkbox"/>
ADVERTISED		<input type="checkbox"/>
LOCATION	
PRINT BUTTON AVAILABILITY CODES		
DIST.	AVAIL. and/or SPECIAL	
G		

Unclassified
Security Classification

14. KEY WORDS	LINK A		LINK B		LINK C	
	ROLE	WT	ROLE	WT	ROLE	WT
Spherical Caps Southwell Plot Instability Critical Load Spherical Shells						

Unclassified
Security Classification

9360-71



DEPARTMENT OF THE ARMY
U. S. ARMY AIR MOBILITY RESEARCH & DEVELOPMENT LABORATORY
EUSTIS DIRECTORATE
FORT EUSTIS, VIRGINIA 23604

This work was carried out under Contract DAAJ02-67-C-0031 with Stanford University.

The data contained in this report are the result of research conducted to investigate the application of the Southwell plot to the interpretation of experimental data on the instability behavior of spherical caps and spherical shells.

The report has been reviewed by this Directorate and is considered to be technically sound. It is published for the exchange of information and the stimulation of future research.

This program was conducted under the technical management of Mr. James P. Waller, Structures Division.

Task 1F162204A17002
Contract DAAJ02-67-C-0031
USAAVLABS Technical Report 69-61
September 1971

INSTABILITY OF SPHERICAL CAPS AND COMPLETE SPHERES

By

Philippe Jacques Jean-Marie Lebouc

Prepared by

Stanford University
Stanford, California

for

EUSTIS DIRECTORATE
U. S. ARMY AIR MOBILITY RESEARCH AND DEVELOPMENT LABORATORY
FORT EUSTIS, VIRGINIA

Approved for public release;
distribution unlimited.

SUMMARY

The general analysis of instability made by Westergaard (Reference 1) in 1922 indicates that the deformation of a body, the initial imperfection, and the critical and actual load levels can be associated by a single law. Southwell (Reference 2), in independent research made in 1932, examined this situation in detail for a column and proposed a method of plotting experimental results for imperfect specimens which could predict the instability load for the perfect column. He indicated in his paper that the process should have a wider content than that in which he worked. Subsequent research has verified this conjecture for a wide range of problems.

This report is concerned with the instability behavior of spherical shells for which, so far as can be traced from a broad literature survey, no application of this technique has been considered. Moreover, it is an area in which the scatter between experimental results is normally great and in which there is still considerable analytical effort being made.

The report demonstrates that the Southwell Plot approach gives an interpretation of experimental data which is consistent with the findings of small displacement computations.

<u>TABLE OF CONTENTS</u>	<u>Page</u>
SUMMARY	iii
LIST OF ILLUSTRATIONS	vi
LIST OF TABLES	ix
LIST OF SYMBOLS	x
INTRODUCTION	1
DETERMINATION OF THE VALUE OF CRITICAL LOAD FOR AN IDEAL SHELL USING A REAL STRUCTURE	3
REMARKS ON THE DISCREPANCY BETWEEN THEORETICAL PREDICTIONS AND EXPERIMENTAL RESULTS	5
INSTABILITY OF SPHERES UNDER VARIOUS LOAD CONDITIONS	8
Spheres Loaded by Uniform External Pressure	8
Spheres Loaded by Normal and Tangential Forces	8
SOUTHWELL APPROACH APPLIED TO KNOWN EXPERIMENTAL DATA	21
Kaplan and Fung's Experimental Data on Spherical Caps	21
Experimental Data of Evan Iwanowski et al on Spherical Caps	37
Ashwell's Experimental Data on Spherical Caps	37
Experiments on a Nickel Sphere	37
REFERENCES	66
DISTRIBUTION	69

LIST OF ILLUSTRATIONS

<u>Figure</u>		<u>Page</u>
1	Scatter of Experimental Data (From SUDAAR 254)	6
2	Data From Kaplan and Fung	7
3	Buckling of a Thin-Walled Spherical Shell Loaded With Uniform External Pressure	9
4	Buckling of a Thin-Walled Spherical Shell Loaded With Uniform External Pressure When Buckling Motion is Restrained by an Interior Mandrel	10
5	Closeup View of Buckle Pattern	11
6	Closeup View of Final Buckle Pattern	12
7	Buckling of a Thin-Walled Spherical Shell by a Force Normal to its Surface	13
8	Buckling Patterns for Thin Spherical Shells Subjected to Various Loading Conditions When Buckle Motion is Restrained by an Interior Mandrel	14
9	Buckle Pattern - Normal Tension Force With External Pressure	15
10	Buckle Pattern - Normal Tension Force After Release of External Pressure	16
11	Buckle Pattern - Surface Shear Force	17
12	Buckle Pattern - Surface Tension Force	18
13	Buckle Pattern - Two Perpendicular Surface Tension Forces	19
14	Buckling Pattern for a Thin-Walled Spherical Shell With a Solid Bottom Half and Tension Applied by Means of an Internal Spherical Cap	20
15	Comparison of Experimental Pressure - Center Deflection Curves With Theoretical Results	22
16	Experimental Pressure - Center Deflection Curves	23
17	Southwell Plot of Specimen 3 (NACA TN 3212).	28
18	Southwell Plot of Specimen 4 (NACA TN 3212).	29
19	Southwell Plot of Specimen 5 (NACA TN 3212).	30

<u>Figure</u>		<u>Page</u>
20	Southwell Plot of Specimen 7 (Kaplan and Fung Data NACA TN 3212)	31
21	Southwell Plot of Specimen 10 (NACA TN 3212)	32
22	Southwell Plot of Specimen 16 (NACA TN 3212)	33
23	Comparison of Theoretical Critical Load and Southwell Values of Buckling (NACA TN 3212)	34
24	Southwell Plot Data From NACA TN 3212 Plot for Theoretical Curve.	35
25	P_{cr} versus λ as Derived From Southwell Plots of Kaplan and Fung's Data (Reference 21).	36
26	Load-Displacement Curves of Spherical Caps Subjected to Internal Pressure and Concentrated Load at the Apex (Loo and Evan Iwanowski, Page 303), Boundary Condition, Edges Clamped	38
27	Southwell Plot of Specimen CUC 037 (Loo and Evan Iwanowski)	44
28	Southwell Plot of Specimen CUC 034 (Loo and Evan Iwanowski).	45
29	Southwell Plot of Spherical Dome Subjected to Uniform Pressure and Normal Concentrated Load at the Apex (Specimen CUC 032 - Loo and Evan Iwanowski)	46
30	Symmetric Mode of Buckling (Evan Iwanowski, Cheng, and Loo, Figure 1A, Page 472) SC 303	47
31	Load-Deflection Curves of a Spherical Dome Subjected to a Concentrated Load at the Apex (Evan Iwanowski, Cheng, and Loo)	48
32	Loo, Cheng, and Evan Iwanowski Data on Spherical Cap Subjected to Concentrated Load at the Apex (Figure 16, SC 303)	49
33	Southwell Plot of Specimen SC 039 (Loo, Cheng, and Iwanowski)	50
34	Southwell Plot of Specimen SC 042 (Loo, Cheng, and Iwanowski)	51
35	Loo, Cheng, and Iwanowski's Data on Spherical Cap - SC 041, $\lambda = 6.3$	52

<u>Figure</u>		<u>Page</u>
36	Data for Symmetrical Cases From Loo, Cheng, and Iwanowski (0) Plus One Point From Ashwell (Δ)	53
37	Ashwell's Experimental Data for a Sphere With Point Load at the Apex	54
38	Ashwell's Experimental Data	56
39	Theoretical Curves of the Critical Load of a Spherical Cap Subjected to a Concentrated Load Versus λ (Geometrical Parameter)	57
40	Radial Displacement Versus External Pressure for Nickel Sphere S958, Test I	58
41	Pressure-Displacement Relationship for Nickel Sphere S958, Location I, Run I, Test II	61
42	Southwell Plot for the Data of Tests on Sphere S958, Location I, Run I, Test II	63
43	Dimple Amplitude Parameter Versus Pressure (Reference Thompson, Figure 5, Page 193)	65
44	Southwell Plot for Thompson's Experimental Data on a Sphere Under External Pressure (Reference 29)	66

LIST OF TABLES

<u>Table</u>		<u>Page</u>
I	Specimen 3 (NACA TN 3212)	24
II	Specimen 4 (NACA TN 3212)	24
III	Specimen 5 (NACA TN 3212)	25
IV	Specimen 7 (NACA TN 3212)	25
V	Specimen 10 (NACA TN 3212, page 56)	26
VI	Specimen 16 (NACA TN 3212, page 56)	27
VII	Theoretical Curve (NACA TN 3212)	27
VIII	Evan Iwanowski and Loo (CUC 037)	27
IX	Evan Iwanowski and Loo (CUC, page 303)	39
X	Evan Iwanowski and Loo (CUC 032, Figure 13)	29
XI	Evan Iwanowski, Cheng and Loo (SC 303)	40
XII	Evan Iwanowski, Cheng and Loo (SC 041, Figure 18)	41
XIII	Evan Iwanowski, Cheng and Loo (SC 042)	42
XIV	Evan Iwanowski, Cheng and Loo	43
XV	Ashwell (Reference 16, Figure 12, Page 60)	55
XVI	Test I - Sphere - S 958	59
XVII	Test II - Sphere - S 958	62
XVIII	Thompson Data	62

LIST OF SYMBOLS

a	base radius of the sphere
E	Young's modulus
b	central height of shell above base plane
P	applied load
P_{cr}	buckling load
t	thickness of the shell
w_o	normal deflection
δ	lateral deflection
λ	defined by equation (3)
v	defined by equation (2)
μ	Poisson's ratio

INTRODUCTION

The behavior of spheres and spherical caps under the action of destabilizing forces is a subject of considerable interest in many areas. This report presents the results of research made to correlate the data obtained in tests with the predictions of theory.

In all research on the stability of bodies, difficulty occurs in the definition of the instability point. Basically, no realistic body can behave in a manner analogous to that described by the analyst. Initial imperfection of shape causes motions to occur from the very onset of load application. These motions increase in magnitude with an increase in load and ultimately cause collapse. That there is an extremely rapid rate of growth of deformation prior to collapse is unquestionable. But the association of this point, obtained for the imperfect body, with the classic critical value for the perfect specimen is virtually impossible. Therefore, effort has been concentrated in a new approach to the interpretation of experimental data. Westergaard (Reference 1), in his general treatment of elastic stability, has suggested that the relationship between deformations and loading actions may be a consistent character for a wide variety of structures and load environments. Southwell (Reference 2), in independent research, explored this situation in depth for the column and presented a powerful tool for interpreting test data for such structures. Other researchers have shown that this approach can be extended to other vehicles. Thus, this report concerns the load-displacement pattern for spheres and spherical caps and attempts to show, from currently existing data and theory, that a 1:1 correspondence can be established.

The theory of instability for spheres and spherical caps was established by Zoelley (Reference 3), Schwerin (Reference 4), and A. Van der Neut (Reference 5). The latter author also developed a general solution for unsymmetrical buckling. Biezeno (Reference 6) presented the analysis for a spherical cap subjected to a concentrated load. This theory is valid within limits which will be defined later. Von Kármán and Tsien (Reference 7) noted the rapid falloff of the load-carrying capacity of thin shells after buckling and reported tests conducted on hemispherical brass shells subjected to external pressure. These experiments were conducted by Sechler and Bollay (Reference 8). Von Kármán and Tsien considered the buckle-dimple as a shallow shell and the buckling motion as a "snap-through" of a spherical cap. From this study, they were led to distinguish an upper-buckling load and a lower-buckling load, now termed the buckling load and postbuckling load, respectively. On this basis, they compared the experimental results of Sechler and Bollay (Reference 8) with their theoretical work. They found good agreement between their predicted postbuckling load and the actual critical load experimentally established by Sechler and Bollay. This practical buckling load was about a quarter of the classical value.

Friedrichs (Reference 9) refined the above theory by using asymptotic expressions to represent the dimple shape. He treated the clamped-edge problem of the dimple as "a boundary layer phenomenon". At the same time, he removed the assumption that the deflection was parallel to the axis of revolution, for this assumption had "an exceedingly strong effect".

Subsequently, Tsien (Reference 10) introduced an energy criterion which predicted a variation of buckling load with test system stiffness. The validity of this criterion as applied to spheres and spherical caps is questionable, as is indicated by the research of Krensk (Reference 11); Carlson, Sendelbeck, and Hoff (Reference 12); and Kaplan and Fung (Reference 13). These direct observations are confirmed by studies on cylindrical shells, such as those reported by Horton and Bailey (Reference 14).

The theory of spherical shells has received much attention during the last twenty years. All large deflection analysis contains the assumption that the buckle has the shape of a spherical cap. The ridge of the buckle has been considered as a "boundary layer phenomenon" by Friedrichs and a yield hinge by Hoff and Soong (Reference 15). The equations have been treated by means of a perturbation solution by Kaplan and Fung (Reference 13) and by a numerical process. Ashwell (Reference 16) developed what he termed a "theory of applicable surfaces" in order to study the problem. Despite these many attempts to match theoretical and experimental work, the disagreement is still large. Fung and Sechler (Reference 17) expressed the view that "In order to bring theory and experiments to complete accord, it would seem more profitable to explore the effects of residual stresses, initial imperfections and dynamic disturbances." It is very difficult to take exception to this statement. Nevertheless, it seems clear that effort must also be extended to derive data for the perfect body from results on imperfect structures. The desirability of establishing the soundness of a theory of perfect structures before extension to the imperfect is undertaken seems to be a logical necessity. The majority of experimental results available today are for shallow spherical caps. Tests of complete spheres are relatively scarce. This is not surprising since the spherical shell is a much more difficult body to fabricate, unless it contains joints or seams which might influence its behavior. Recent development in plating technology has improved this state immeasurably.

An important series of tests was made by Kaplan and Fung (Reference 13). They tested shallow spherical magnesium caps under uniform external pressure using either air or oil pressure loading. Fung and Sechler (Reference 17) discussed this work and denied the validity of the perturbation technique used in the theoretical computation.

Later, Ashwell (Reference 16) conducted four point-loading experiments on aluminum alloy shells in order to determine the load-deflection relationship. He compared his experimental results with Tsien and Biezeno's theories.

Thompson (Reference 18) tested two complete polyvinyl chloride spheres under uniform external pressure. Finally, Loo and Evan Iwanowski (Reference 19) studied experimentally the deformations and collapse of spherical caps subjected to concentrated point load and uniform pressure. The work of Carlson, Sendelbeck, and Hoff is a genuine contribution to research on the complete sphere and will be discussed later. The basis for the present report is provided by the experiments of Ashwell (Reference 16); Fung and Kaplan (Reference 13); Thompson (Reference 18); Loo and Evan Iwanowski (Reference 19 and 20).

DETERMINATION OF THE VALUE OF CRITICAL LOAD FOR AN IDEAL SHELL USING A REAL STRUCTURE

As far as the method of experimentally determining the critical load for a perfect sphere or a spherical cap using a realistic specimen has been derived, it is possible that the statistical approach developed by Horton and Durham (Reference 21) for cylinders could be applied. Certainly, spherical shells can be completely filled with buckles provided they have an internal mandrel. This is clearly seen from Figure 4. However, the purpose of this study is much broader than the consideration of instability under uniform external pressure. Thus, since the statistical technique referred to is limited by the need for a whole population, it is not considered here. Instead, attention is directed to the possibility that the load-displacement behavior at a well-chosen point on the surface of the shell will enable the critical value to be determined by application of the so-called Southwell Plot.

The literature contains many examples of applicability of this process to a wide range of problems. These are discussed in detail for column and plate structures by Horton, Cundari, and Johnson (Reference 22). Donnell (Reference 23) has investigated the possible use of the technique in the case of cylinders. Flugge (Reference 24), in his textbook on shells, indicates that he and his co-workers have had success in such applications. However, he cautions that the location of the displacement transducer must be chosen with great care.

Currently available test data on spheres under various load conditions have been examined to determine whether or not any of these data could be analyzed using this technique. The results of the study are presented here.

Basically, the process depends upon the fact that, in many cases, the relationship between the initial imperfection, the displacement under load, the load value, and the classical instability can be expressed approximately in the form

$$\delta \left(\frac{P_{cr}}{P} - 1 \right) = \text{constant} \quad (1)$$

This is the equation of a hyperbole. If the variables are altered from P and δ to δ/P and δ , this equation can be rewritten as

$$\nu P - \delta = \text{constant} \quad (2)$$

which represents a straight line whose slope is the critical load. The specimen imperfection is defined by the value of the constant.

In many cases, the law expressed in Equation (1) must be modified as follows:

$$\delta \left(\frac{P_{cr}}{P} - 1 \right) (\lambda) = \text{constant} \quad (3)$$

where λ is a parameter dependent upon the quality of the specimen and the motion under load.

This parameter must be very close to unity if the method is to produce good results. Consequently, the range of applicability might be severely restricted.

REMARKS ON THE DISCREPANCY BETWEEN THEORETICAL
PREDICTIONS AND EXPERIMENTAL RESULTS

Generally speaking, analytical studies are concerned with perfect bodies of specimens with idealized imperfections acted upon by accurately defined loadings. On the other hand, experimental studies must be made on realistic structures under imperfectly controlled load systems. The problems caused by these differences are accentuated by the fact that the boundary conditions prescribed for theoretical study are rarely, if ever, those attainable in the laboratory. Thin shell bodies of all types appear to be remarkably sensitive to these several deviations from ideal, and it is customary to find that test data on such vehicles are at variance with prediction. While theoreticians have striven to widen the basis of these analyses by taking into account deviations of the specimen loading systems and boundaries from the ideal, experimentalists have attempted to improve the geometric and mechanical qualities of their test specimens and to control the test environment more vigorously. In shell structure tests, several experimentalists have been able to develop their techniques of manufacture and testing to such an extent that they have been able to generate extremely high values of tests to theoretical loads. For example, in the case of circular cylindrical shells in axial compression, Tennyson (Reference 26) has shown that it is possible to develop a buckling load of the ideal of 90% of the classic value using a near-perfect specimen, while similar results have been obtained by Carlson, Sendelbeck, and Hoff (Reference 12) for accurate spheres under external pressure loading. These high values of load are the exception rather than the rule.

As already implied, the low values of critical loads are ascribable to specimen or loading imperfections. Generally, in bodies of single curvature, these do not appear to have any pronounced influence on the shape of buckles, but in spherical shells this does not appear to be the case. Spherical shells, particularly under point loads, will buckle in both symmetric and asymmetric patterns. There is some evidence presented later in the report that, if the buckle motion versus load history is considered, then in those cases of symmetrical distortion, the load-displacement curve will be hyperbolic at the buckle center. If this fact is used in a Southwell fashion, the critical load levels determined from slope considerations will be more consistent with prediction than those determined by other means. However, in other cases, in which the distortions are not symmetric, the load-displacement relationships may not be hyperbolic, and, indeed, they frequently seem to differ in form among themselves. Thus, there is no possibility of a Southwell interpretation in many cases, unless it is possible to make observations at a number of points and to perform a harmonic analysis.

The wide scatter that is normally experienced is very evident in Figures 1 and 2.

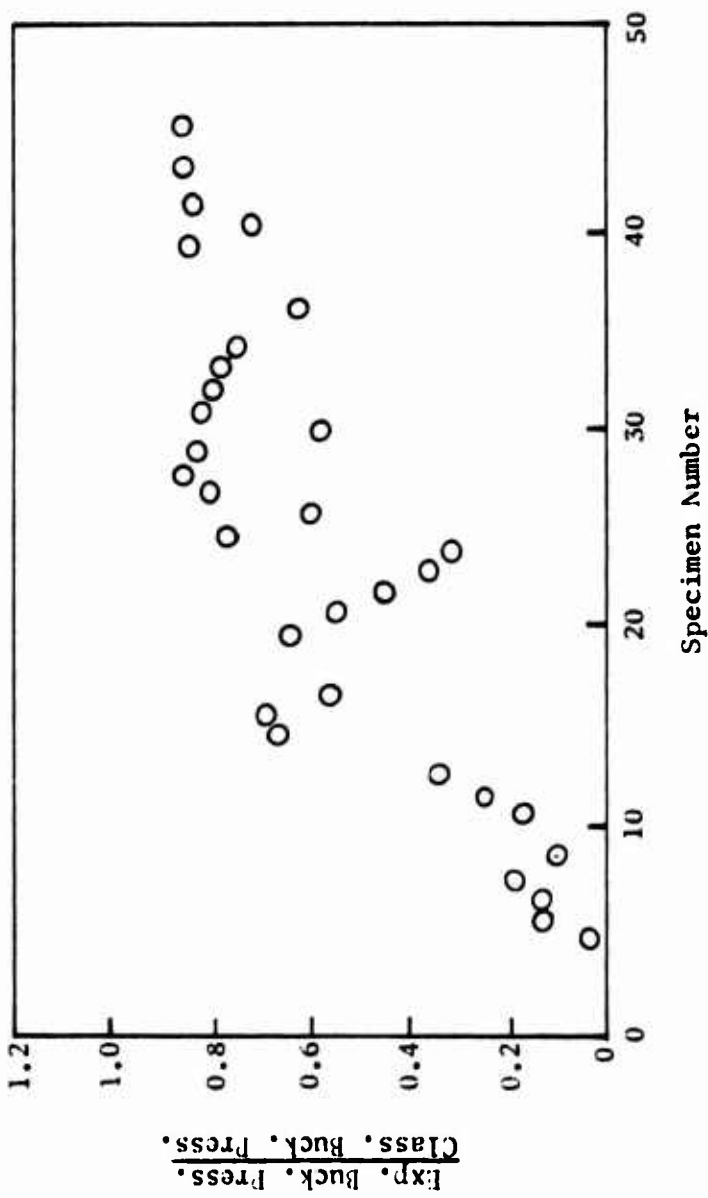


Figure 1. Scatter of Experimental Data (From SUDAAR 254).

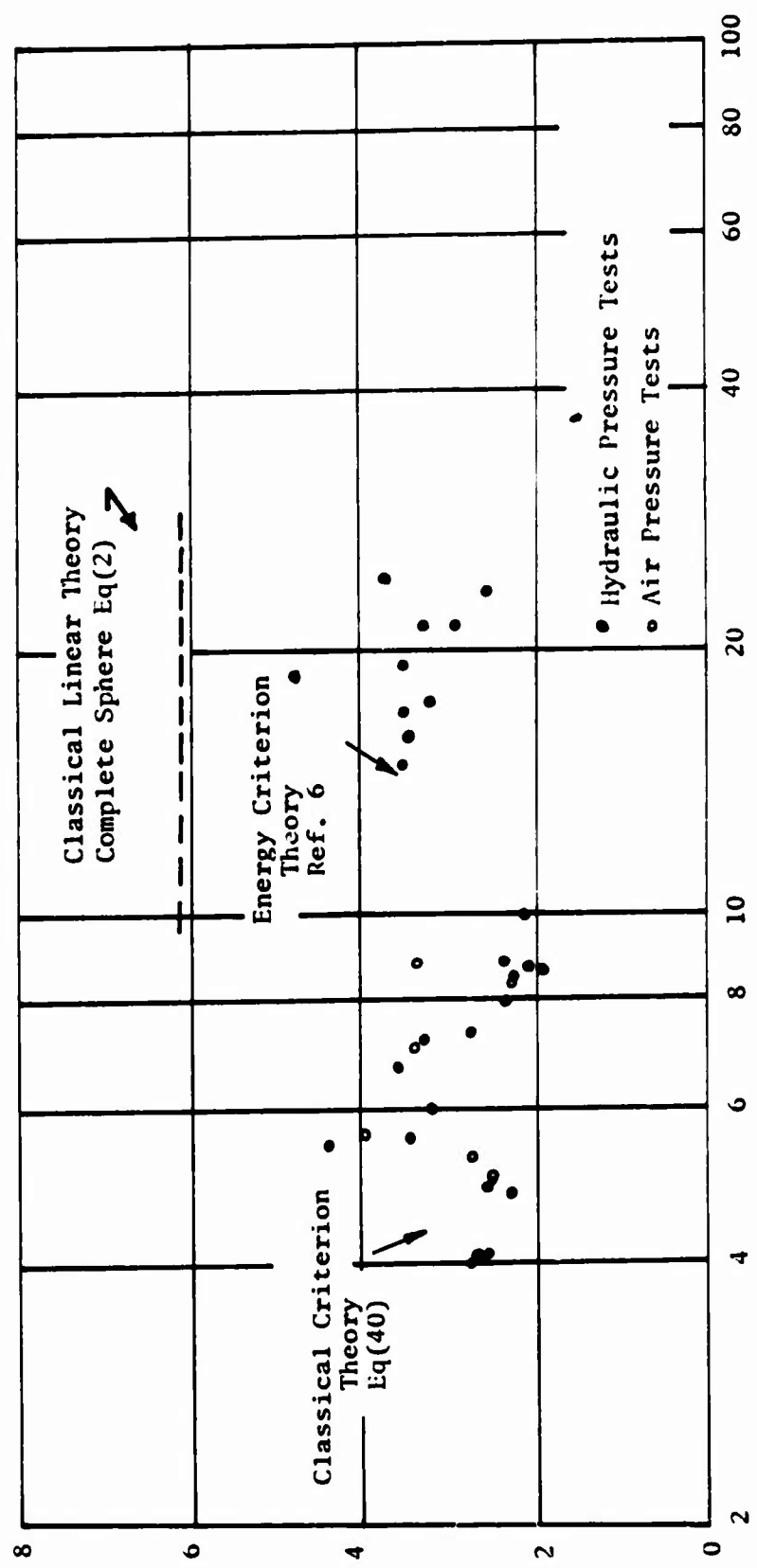


Figure 2. Data From Kaplan and Fung (NACA TN 3212 References Are as Per This Report).

INSTABILITY OF SPHERES UNDER VARIOUS LOAD CONDITIONS

SPHERES LOADED BY UNIFORM EXTERNAL PRESSURE

The instability of spheres loaded in this fashion is very dynamic. The buckle develops at the weakest point, frequently at the junction of the sphere with the tube used for evacuation, because the reinforcement needed at this point induces higher stresses and bending moment. The buckle pattern is shown in Figure 3.

The buckle motion, which is very hard to follow, can be restrained by an interior mandrel, as shown in Figures 4, 5, and 6.

When this is done, it is seen that circular indentations are formed. These grow in size and coalesce into a pattern of hexagons and pentagons as the pressure increases. The gap between specimen and mandrel decides not only the size and amplitude of the buckle but also whether or not there will be plastic stresses in the fold lines along their common boundaries.

The technique for electrodepositing spheres on wax mandrels was developed by Sendelbeck (Reference 25).

SPHERES LOADED BY NORMAL AND TANGENTIAL FORCES

In Figure 7, we can see the buckling pattern developed on a sphere by a normal force. The buckle develops in the neighborhood of the point of application of the force. Figures 8, 9, 10, 11, 12, 13, and 14 show a spherical shell with internal mandrel subjected to various loading conditions.

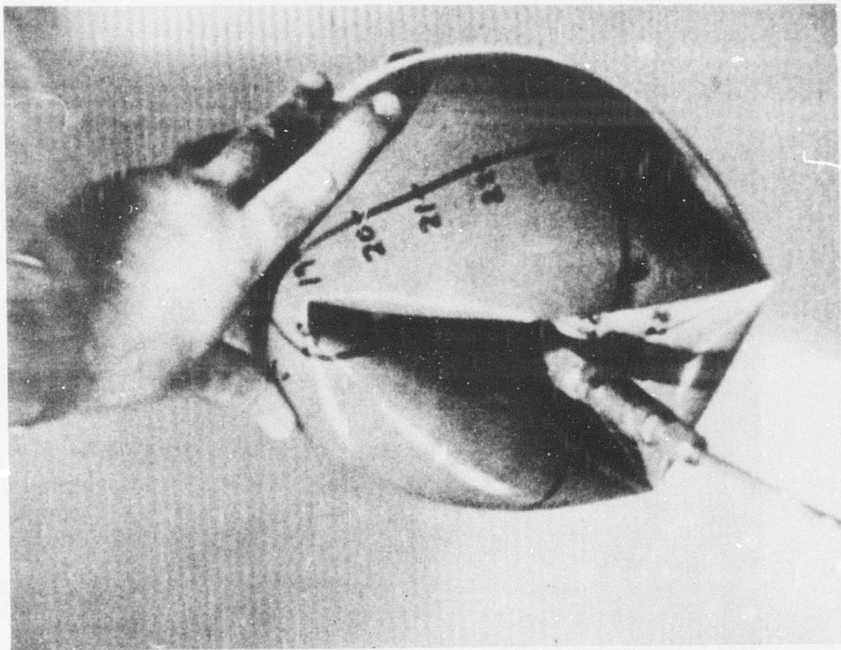


Figure 3. Buckling of a Thin-Walled Spherical Shell
Loaded With Uniform External Pressure.

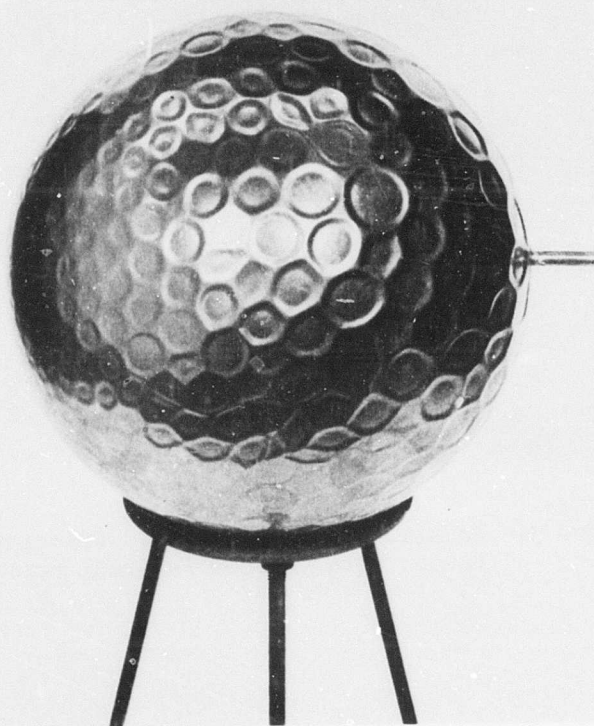


Figure 4. Buckling of a Thin-Walled Spherical Shell Loaded With Uniform External Pressure When Buckling Motion is Restrained by an Interior Mandrel.

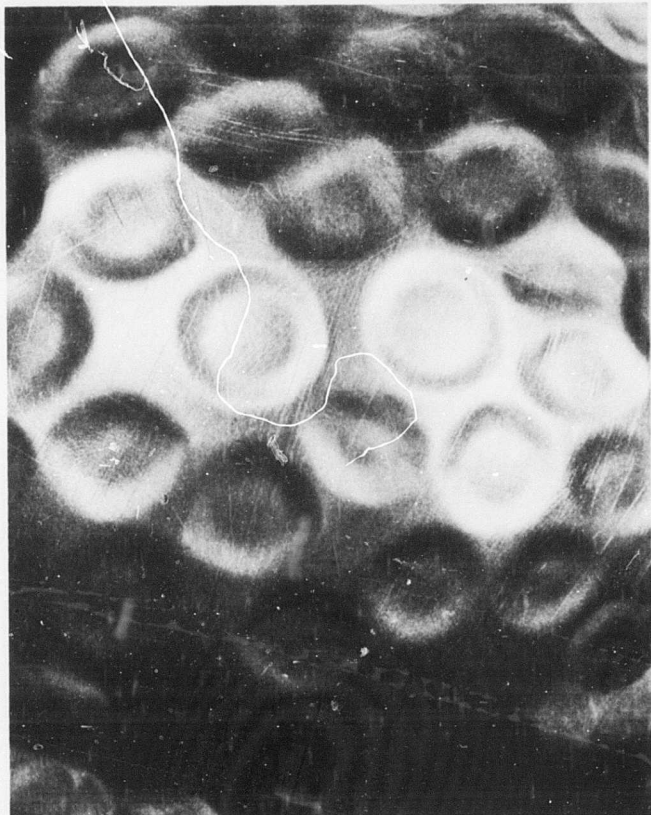


Figure 5. Closeup View of Buckle Pattern.

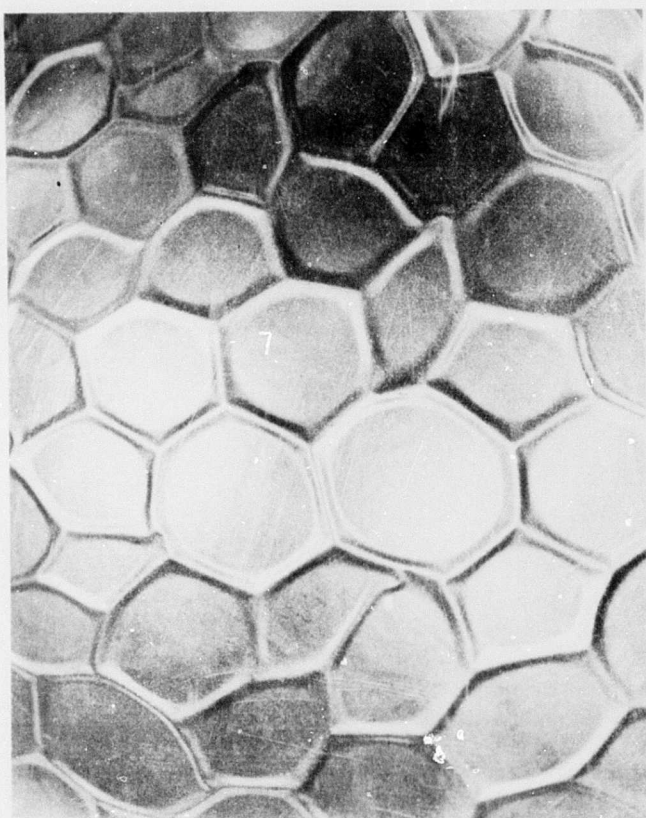


Figure 6. Closeup View of Final Buckle Pattern

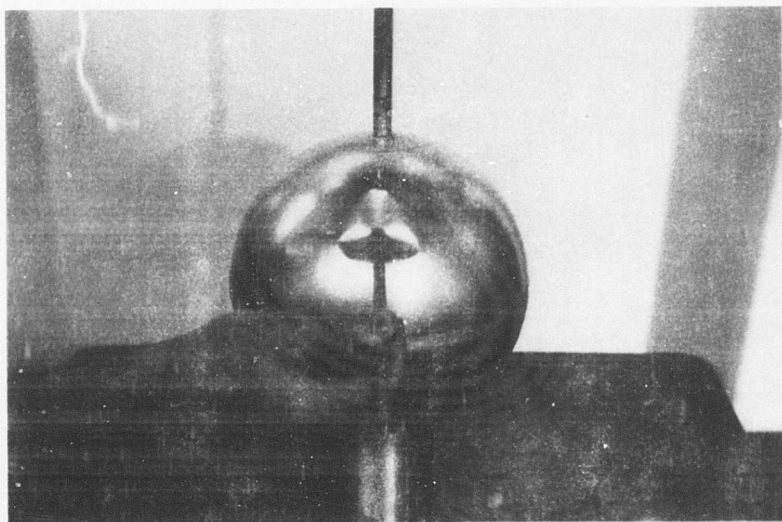
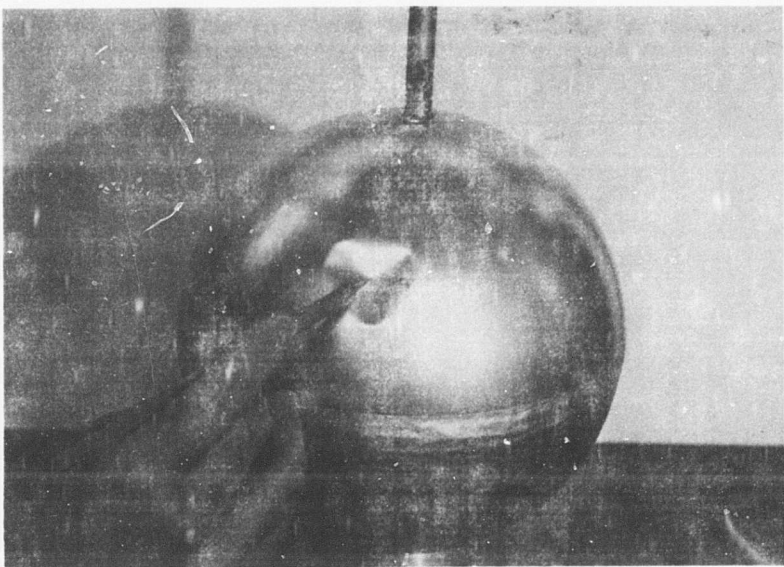


Figure 7. Buckling of a Thin-Walled Spherical Shell by a Force Normal to its Surface.

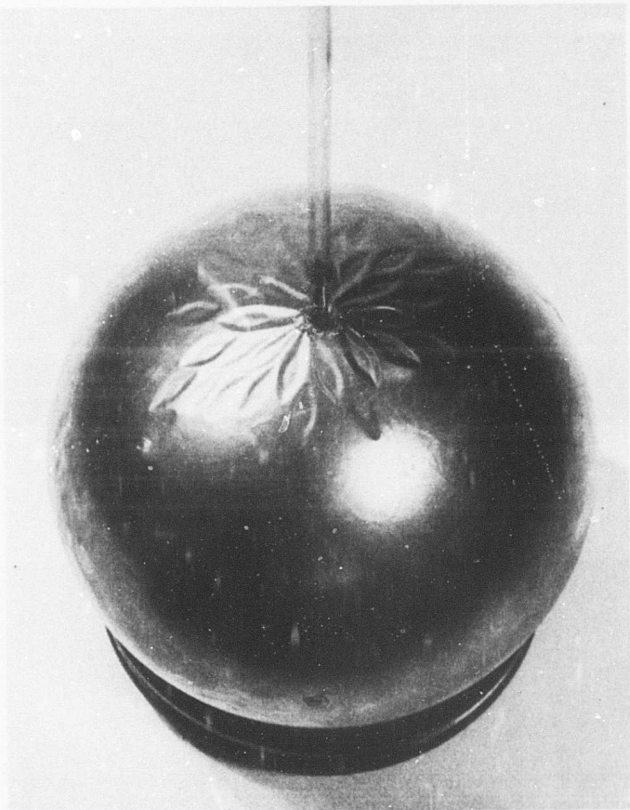


Figure 8. Buckling Patterns for Thin Spherical Shells Subjected to Various Loading Conditions When Buckle Motion is Restrained by an Interior Mandrel.

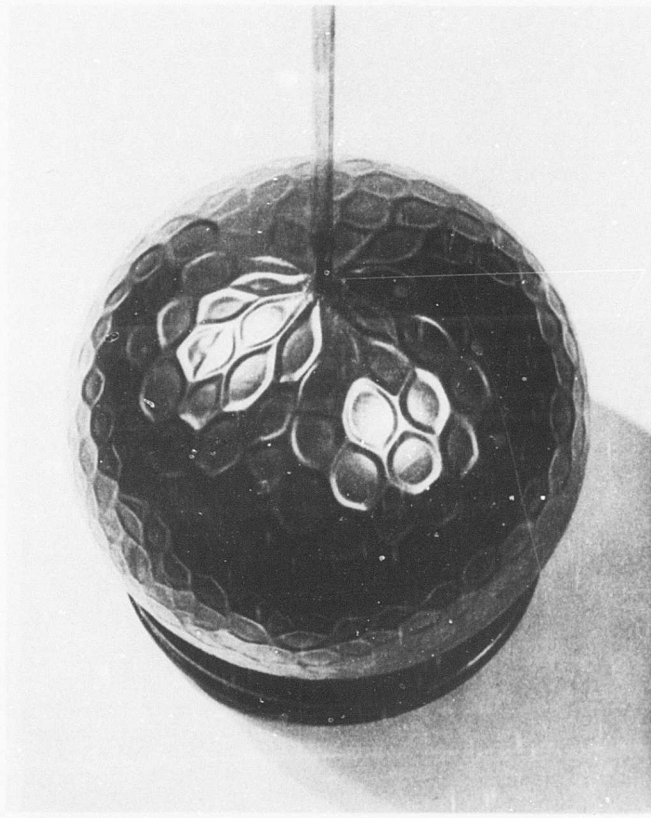


Figure 9. Buckle Pattern - Normal Tension Force
With External Pressure.

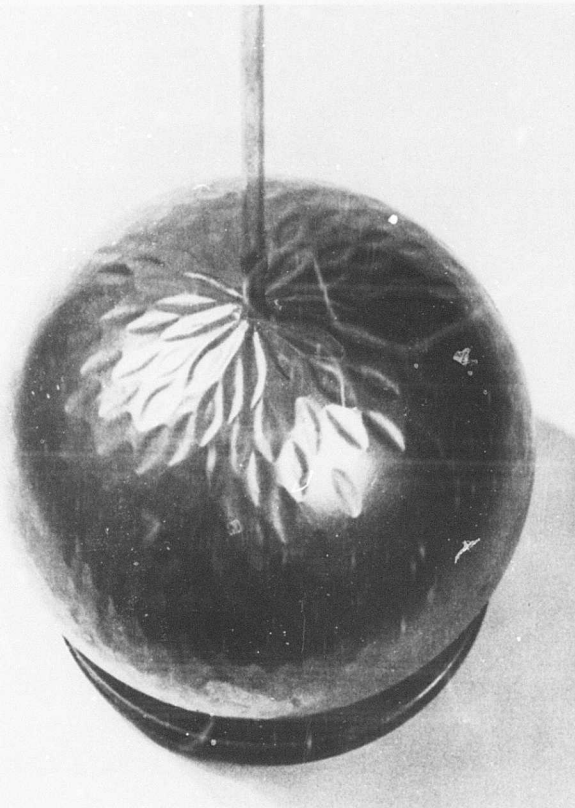


Figure 10. Buckle Pattern - Normal Tension Force After Release of External Pressure.

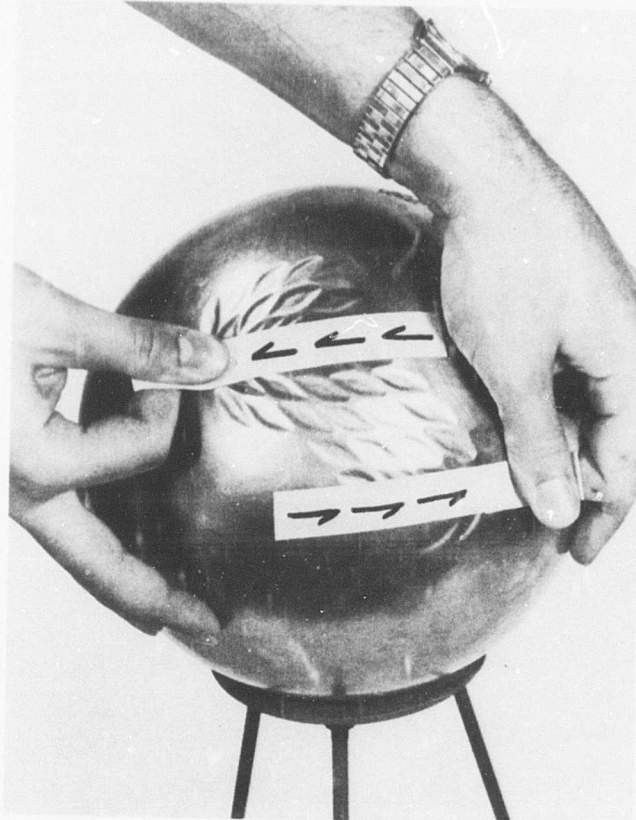


Figure 11. Buckle Pattern - Surface Shear Force.

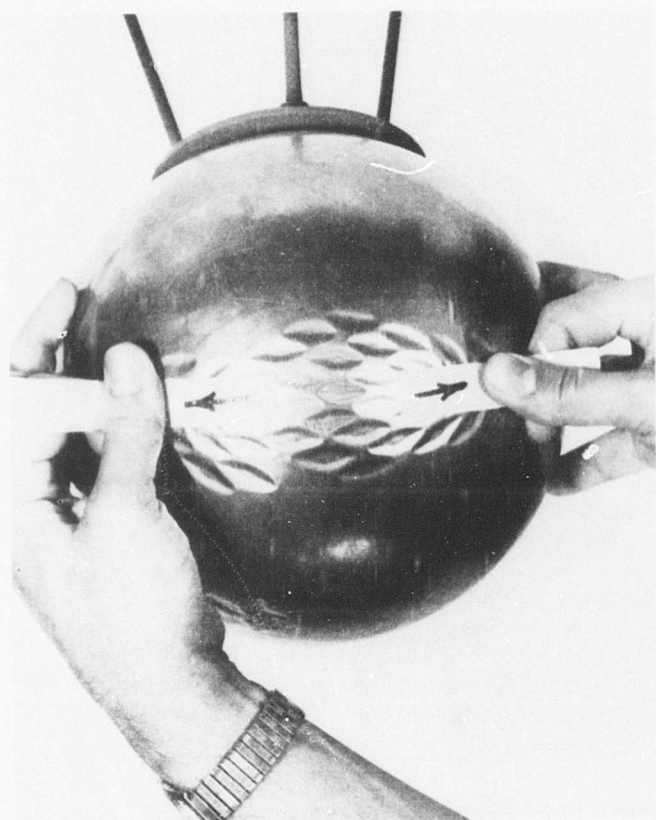


Figure 12. Buckle Pattern - Surface Tension Force.

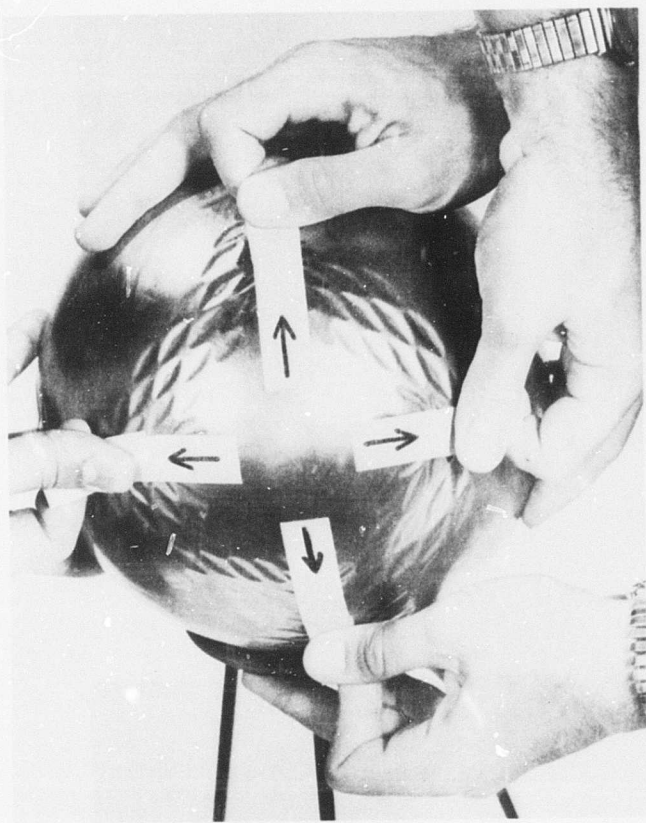


Figure 13. Buckle Pattern - Two Perpendicular Surface Tension Forces.

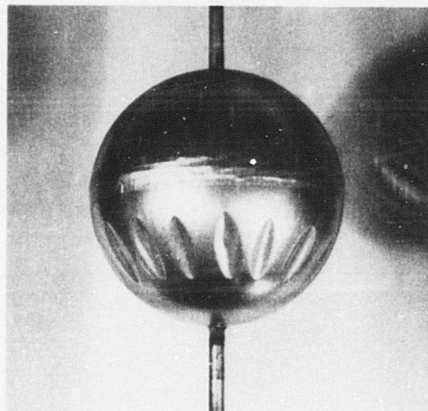
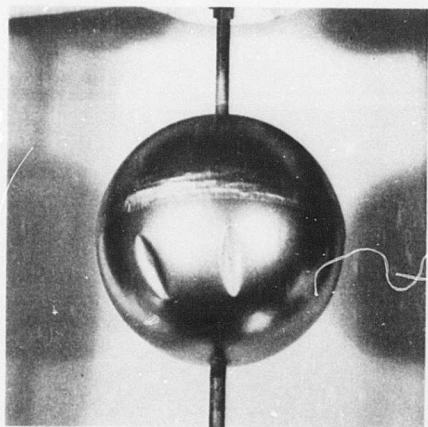


Figure 14. Buckling Pattern for a Thin-Walled Spherical Shell With a Solid Bottom Half and Tension Applied by Means of an Internal Spherical Cap.

SOUTHWELL APPROACH APPLIED TO KNOWN EXPERIMENTAL DATA

KAPLAN AND FUNG'S EXPERIMENTAL DATA ON SPHERICAL CAPS

The pressure deflection curves obtained by Kaplan and Fung (Reference 13) are reproduced in Figures 15 and 16, from which the load-displacement curves of the specimens 3, 4, 5, 7, 10, and 16 have been selected. In Tables I, II, III, IV, V, and VI, the ratios of the displacement to the load, corresponding to each of the above-mentioned specimens, have been computed. In Figures 17, 18, 19, 20, 21, and 22, the deflection w_0 versus the ratio w_0/P has been plotted. It is seen that straight lines are obtained.

From these figures, the slope of the straight lines has been computed. The following values were obtained:

	<u>Slope</u>		<u>Slope</u>
Specimen 3	15.5	Specimen 7	72.5
Specimen 4	34	Specimen 10	182.0
Specimen 5	41	Specimen 16	417

The first of these values have been plotted in Figure 23, which is the theoretical curve of buckling load:

$$P_{cr} = \frac{1 - \mu^2}{E} \left(\frac{a}{t} \right)^4 q \quad \text{versus} \quad \lambda = 2 \left[3(1 - \mu^2) \right]^{\frac{1}{4}} \left(\frac{h}{t} \right)^{\frac{1}{2}}$$

obtained by Kaplan and Fung (Reference 13).

We can observe from this figure that there is very good agreement between the Southwell determination of the buckling load for the ideal specimen and the classical determination of the buckling load.

However, it must be noted that the theoretical load-displacement curve by Kaplan and Fung (Figure 15) for $\lambda = 4$ yields a straight line also, as computed in Table VII and shown in Figure 24. But the critical load given as the slope of this straight line does not agree with the theoretical curve of critical load versus λ (Figure 23).

Thus, one can establish the Southwell analysis of experimental buckling as a criterion for the validity of a theory; i.e., a theory which yields a Southwell plot for a theoretical load-displacement curve whose slope is close to the theoretical value of buckling (such a theory is valid).

The remaining point cannot be correlated with Kaplan and Fung's computation since their values of λ are outside the range covered by the analysis. However, if all of the Southwell-derived critical loads are plotted versus λ on a common plot, it is readily apparent that they are of the same family. This is clearly shown in Figure 25.

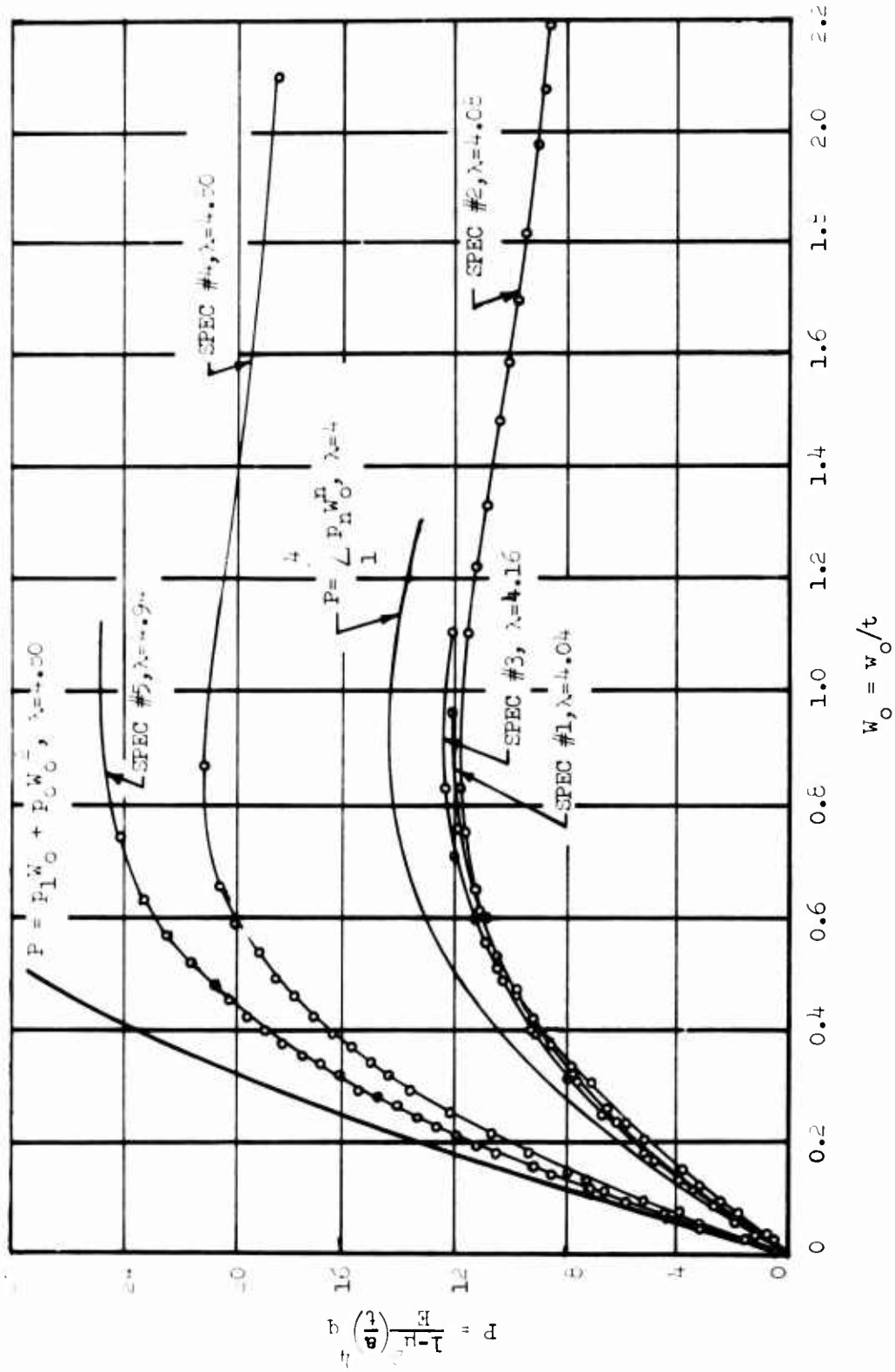


Figure 15. Comparison of Experimental Pressure - Center-Deflection Curves With Theoretical Results.

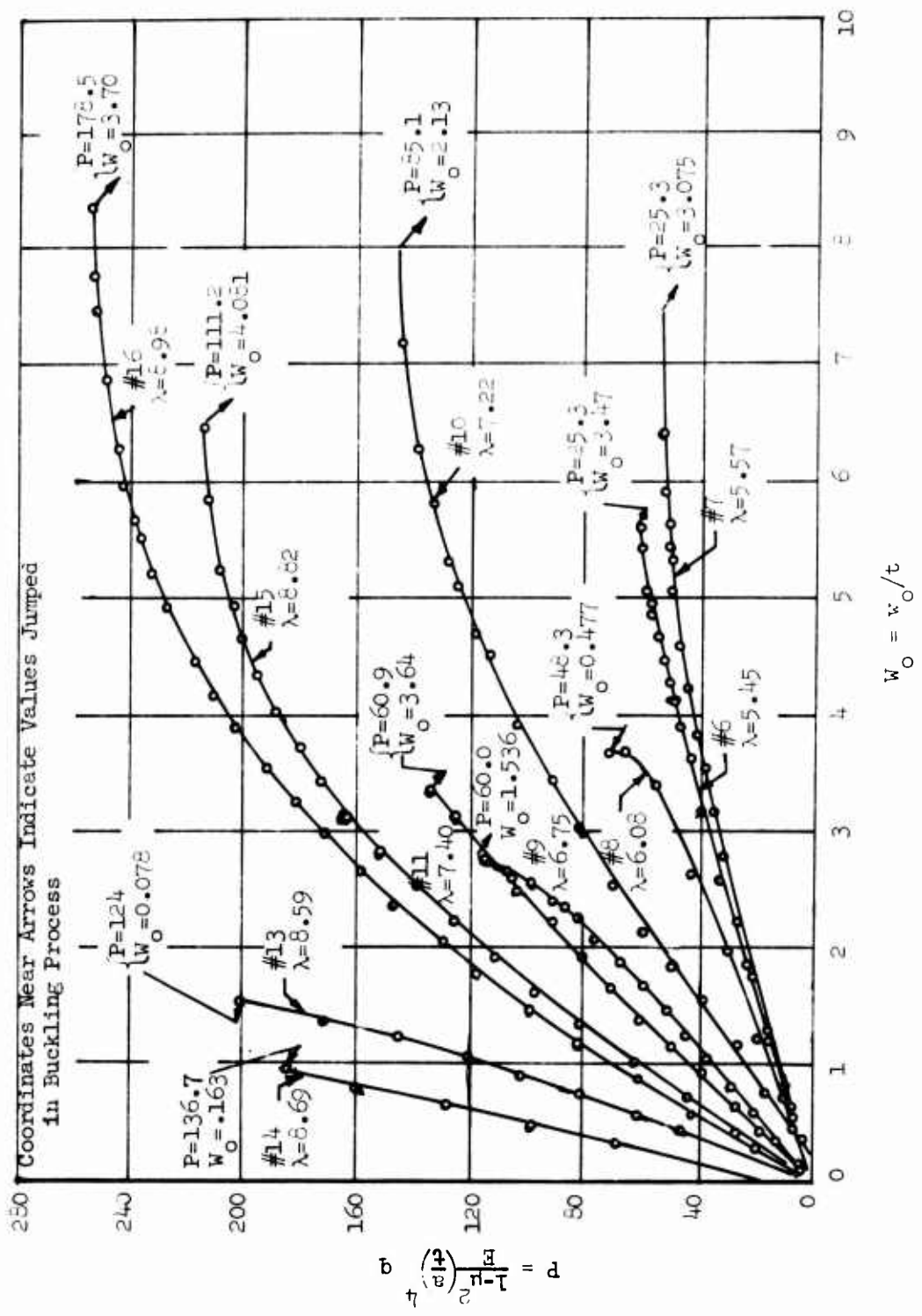


Figure 16. Experimental Pressure - Center-Deflection Curves.

TABLE I. SPECIMEN 3 (NACA TN 3212)

$\lambda = 4.16$		
$P_{cr} = 15.5$		
w_o	P	w_o/P
.888	12.35	.0718
.84	12.2	.0688
.706	11.85	.0596
.593	11.2	.053
.569	11	.0517

TABLE II. SPECIMEN 4 (NACA TN 3212)

$\lambda = 4.8$		
$P_{cr} = 34$		
w_o	P	w_o/P
.746	20.85	.0358
.635	20.3	.0312
.578	19.5	.0296
.525	18.7	.0281
.460	17.6	.0261
.378	15.8	.0239

TABLE III. SPECIMEN 5 (NACA TN 3212)

w_o	P	w_o/P
.633	23.3	.0272
.578	22.3	.0259
.525	21.6	.0243
.460	20.1	.0229
.378	18.1	.0209
.292	15.3	.0192

TABLE IV. SPECIMEN 7 (NACA TN 3212)

w_o	P	w_o/P
.7	54.2	.0129
.65	53.5	.0122
.6	52.0	.0115
.55	51.1	.0108
.5	49.5	.0101
.45	46.5	.0096

TABLE V. SPECIMEN 10 (NACA TN 3212, Page 56)

$\lambda = 7.22$		
w_o	P	w_o/P
.8	148	.0054
.75	147	.00510
.7	144.5	.00485
.65	142	.00455
.6	139	.00430

TABLE VI. SPECIMEN 16 (NACA TN 3212, Page 56)

$\lambda = 8.98$		
w_o	P	w_o/P
.4	206	.00194
.45	218	.00206
.5	229	.00218
.55	239	.00230
.6	243	.00242
.65	250	.00260
.7	252	.00218

TABLE VII. THEORETICAL CURVE (NACA TN 3212)

$\lambda = 4$		
w_o	P	w_o/P
.746	13.9	.0545
.634	13.3	.0476
.578	12.6	.046
.536	12.15	.0441
.460	11.2	.0412
.377	9.995	.0319

TABLE VIII. EVAN IWANOWSKI AND LOO (CUC 037)

δ	P	δ/P
.8	1.46	.549
.7	1.43	.489
.6	1.39	.432
.5	1.345	.372
.4	1.3	.308

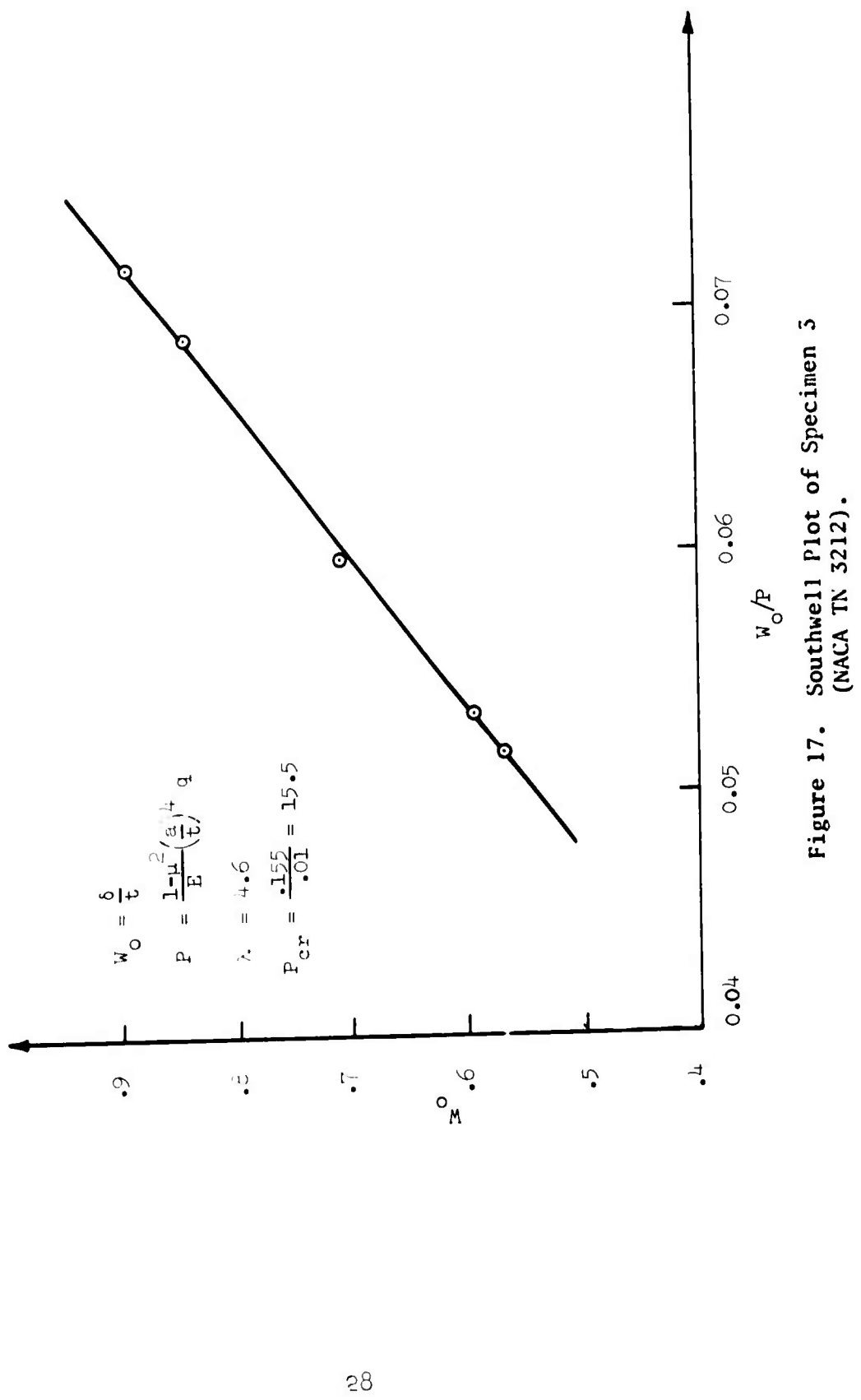


Figure 17. Southwell Plot of Specimen 5
(NACA TN 3212).

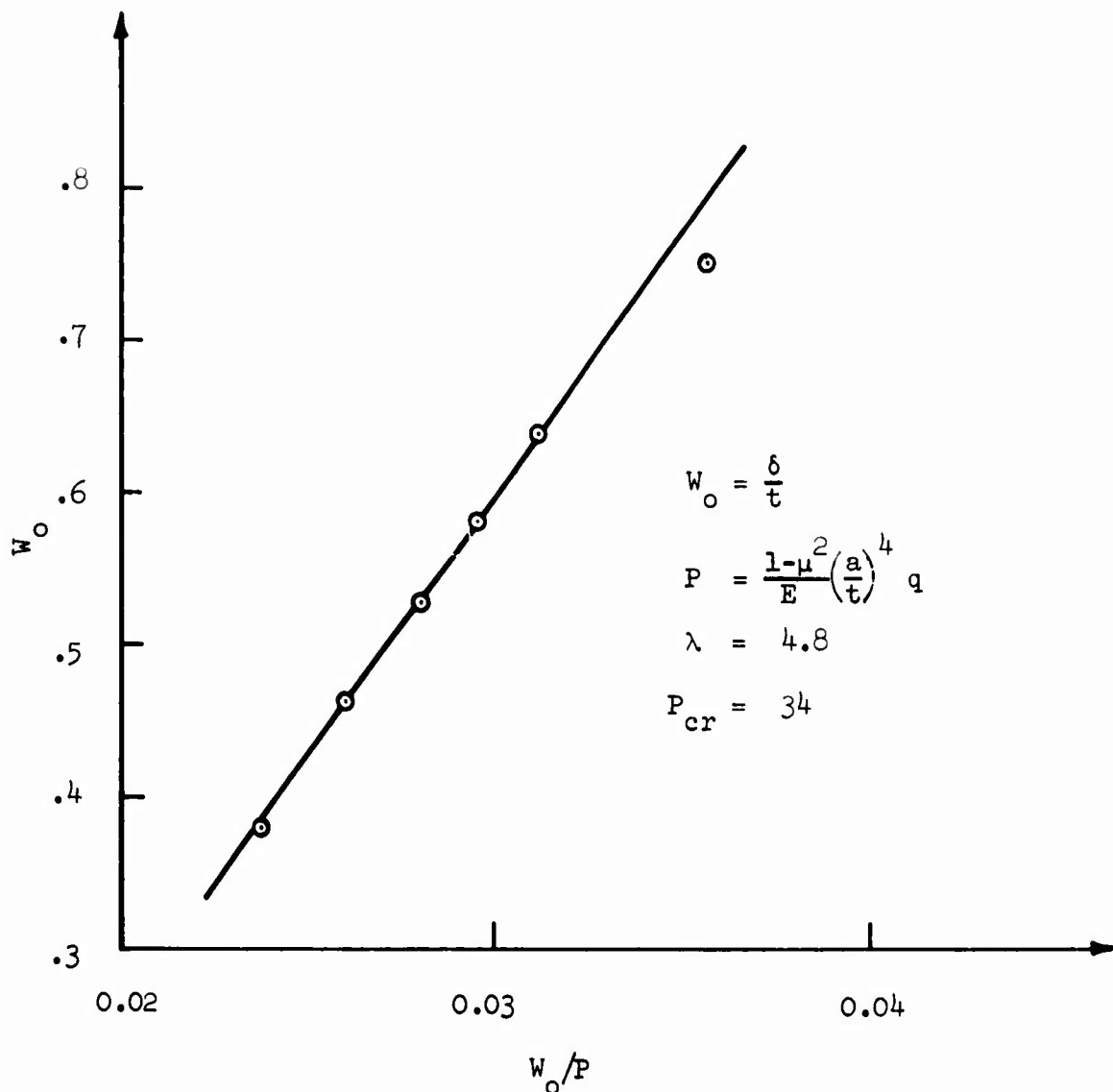


Figure 18. Southwell Plot of Specimen 4 (NACA TN 3212).

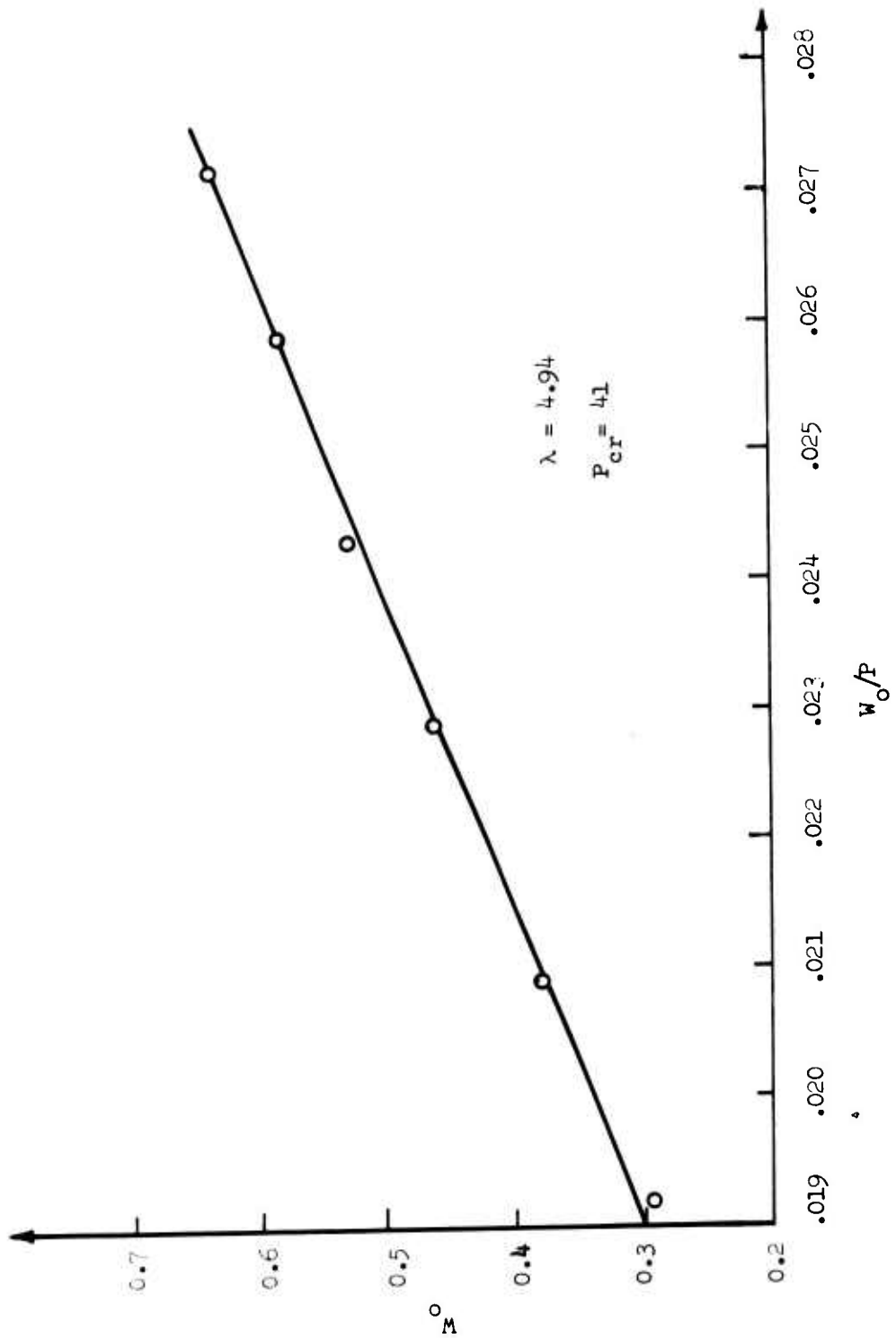


Figure 19. Southwell Plot of Specimen 5 (NACA TN 3212).

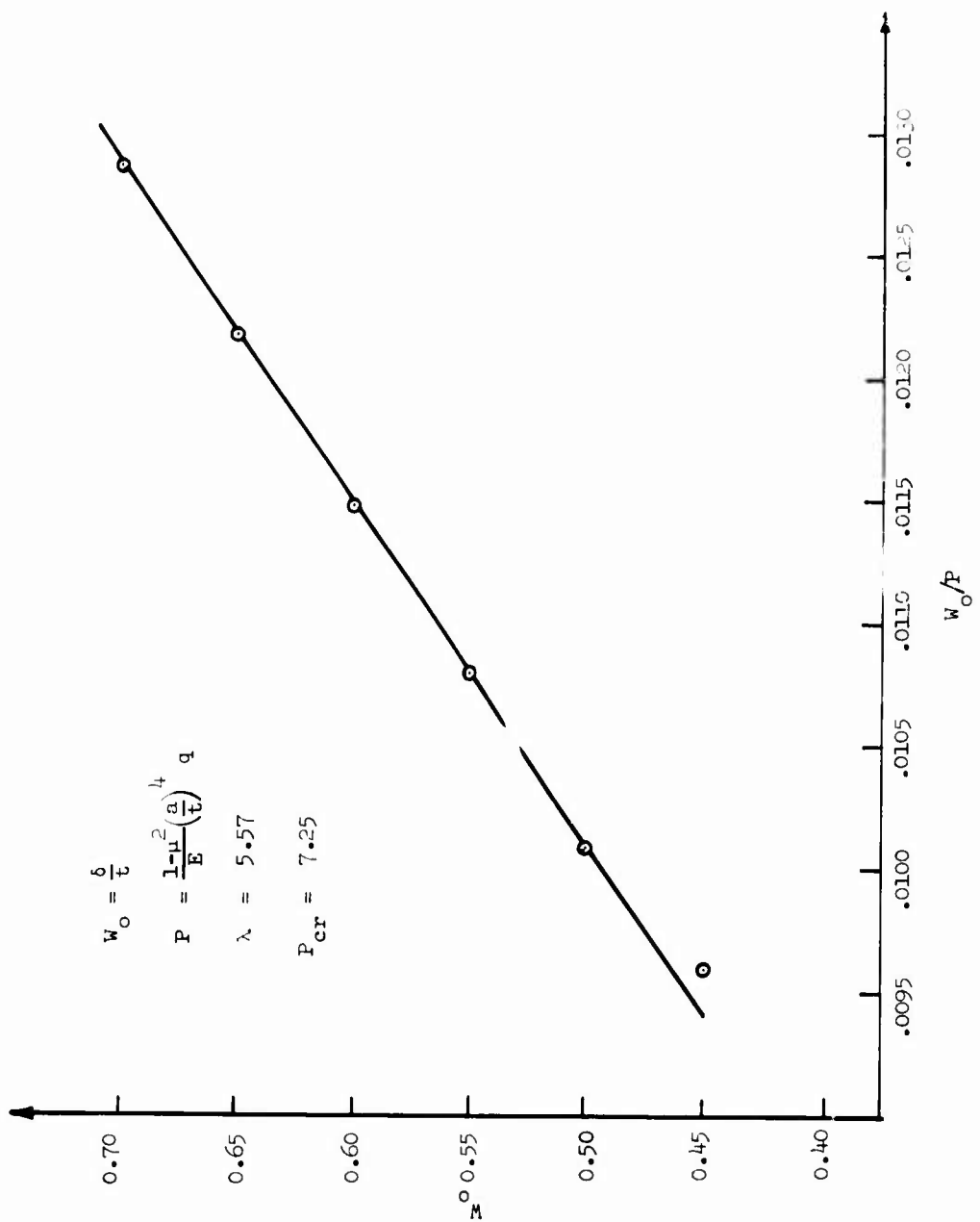


Figure 20. Southwell Plot of Specimen 7 (Kaplan and Fung Data, NACA TN 3212).

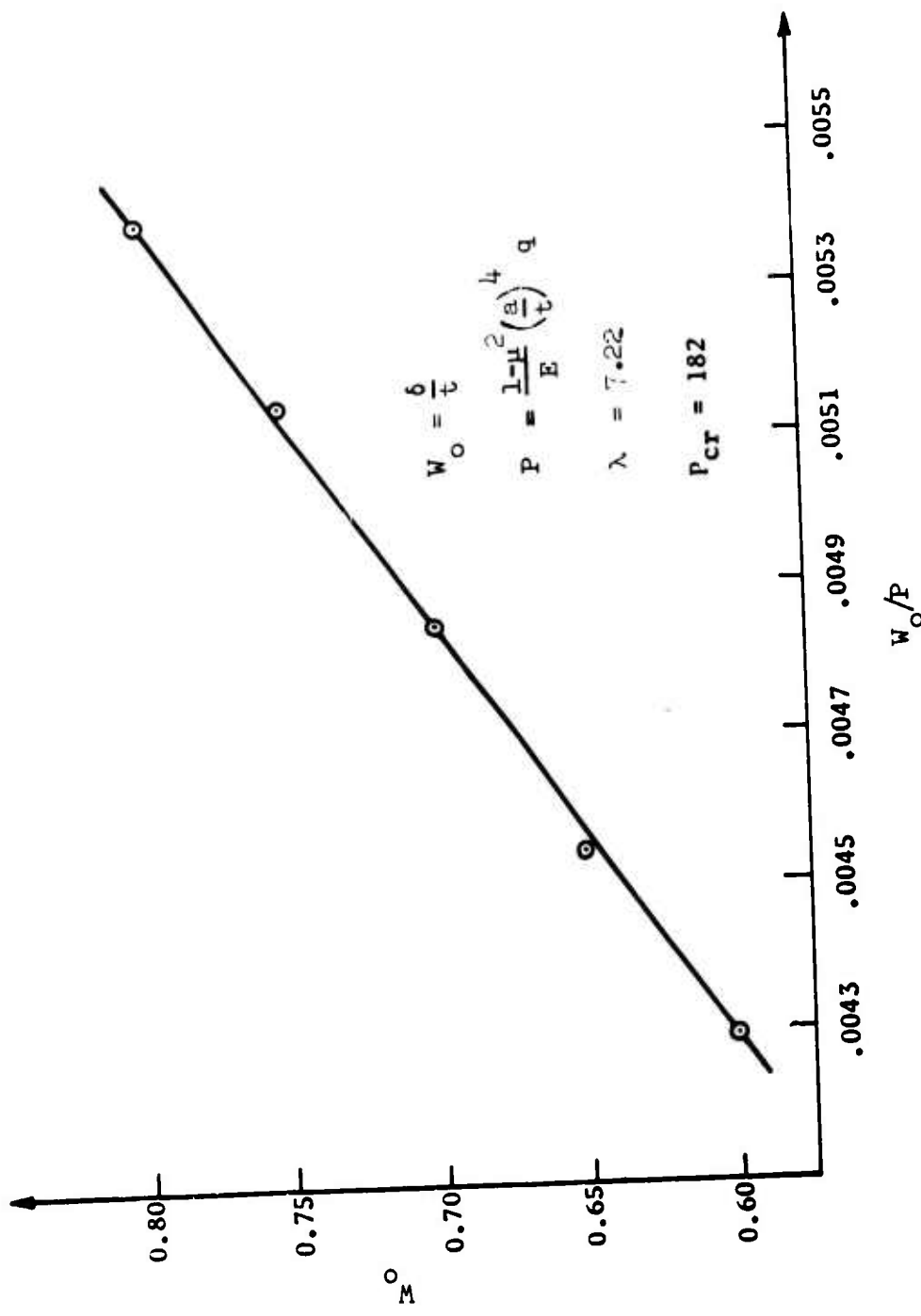


Figure 21. Southwell Plot of Specimen 10 (NACA TN 3212).

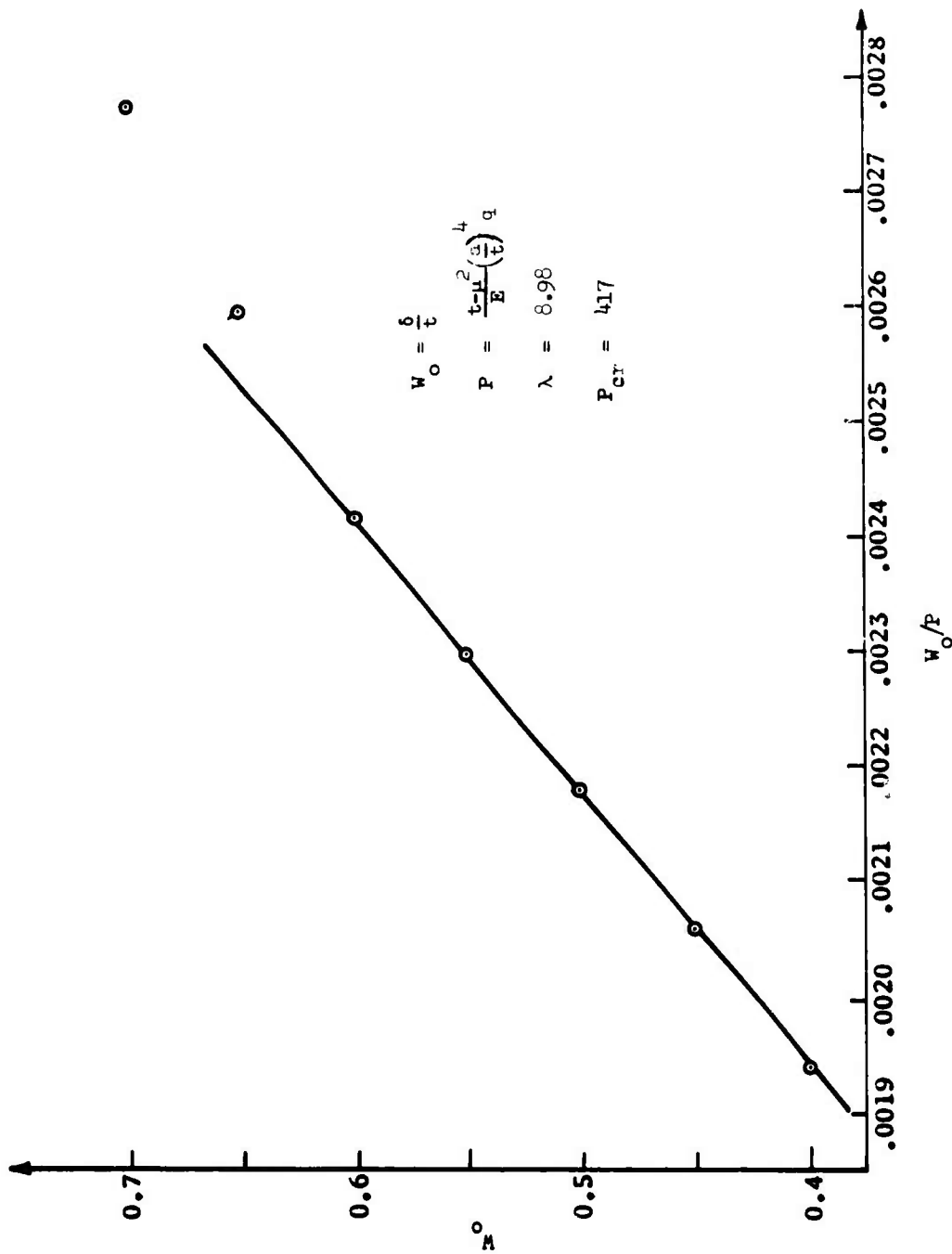


Figure 22. Southwell Plot of Specimen 16 (NACA TN 3212).

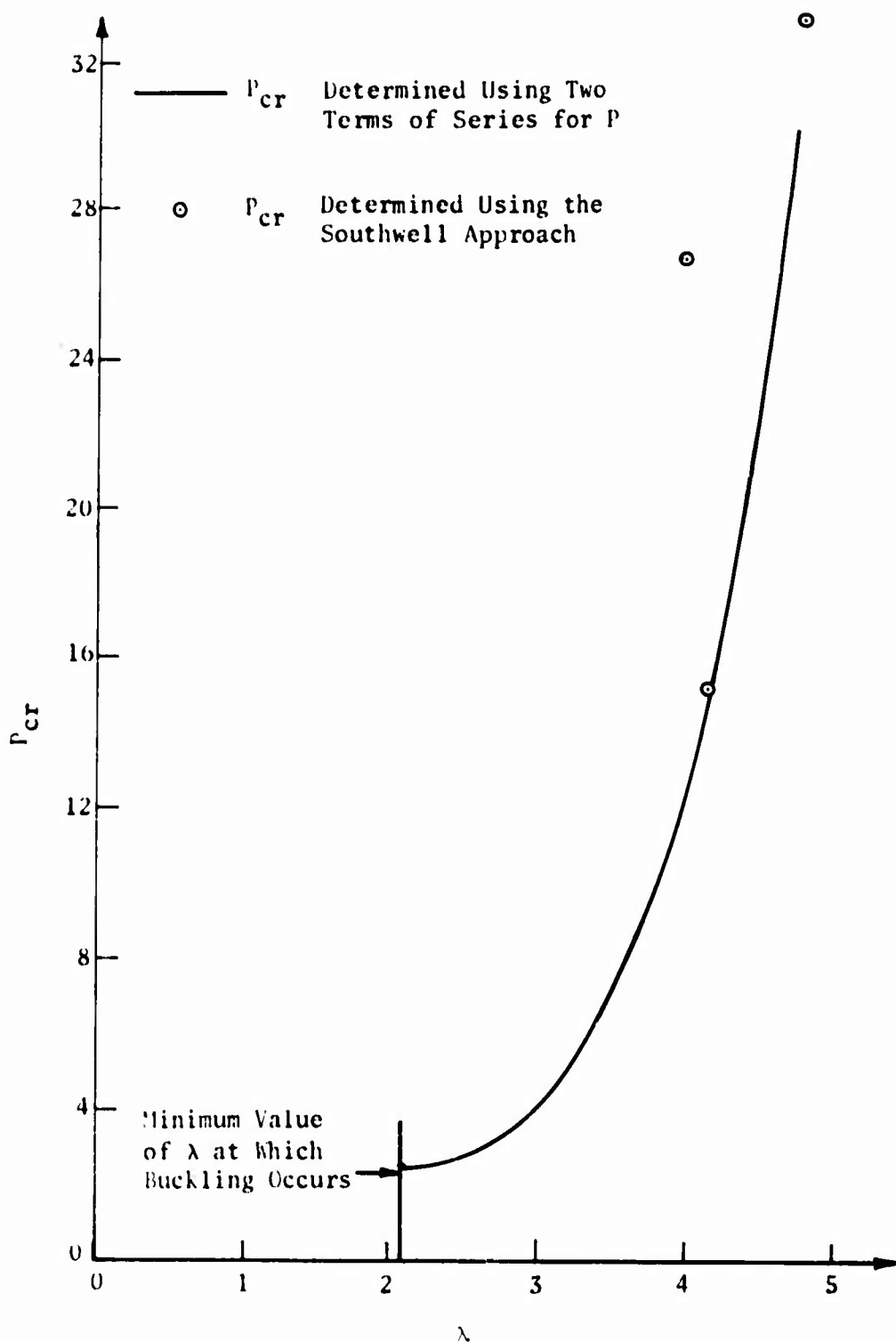
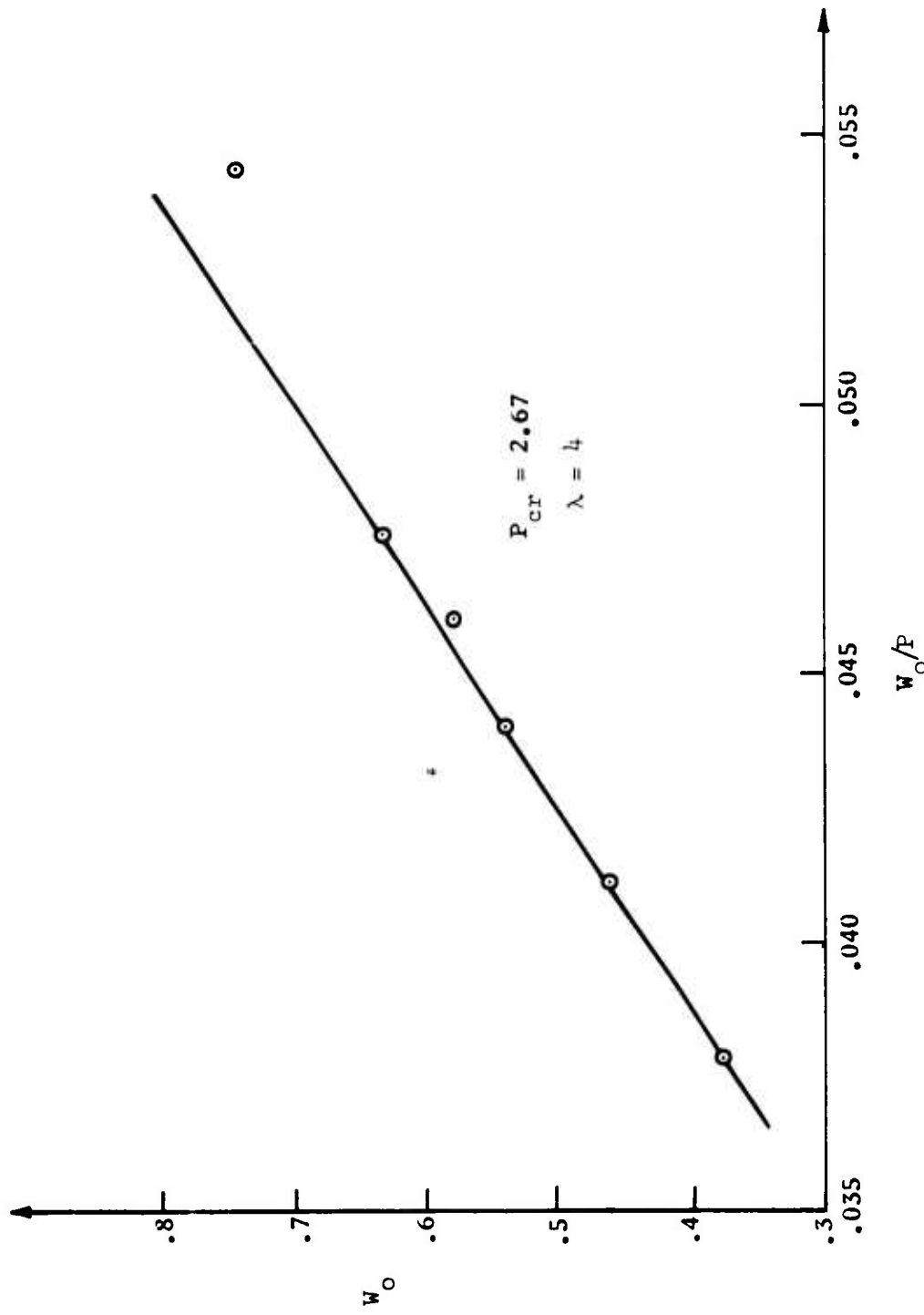


Figure 23. Comparison of Theoretical Critical Load and Southwell Values of Buckling (NACA TN 3212).



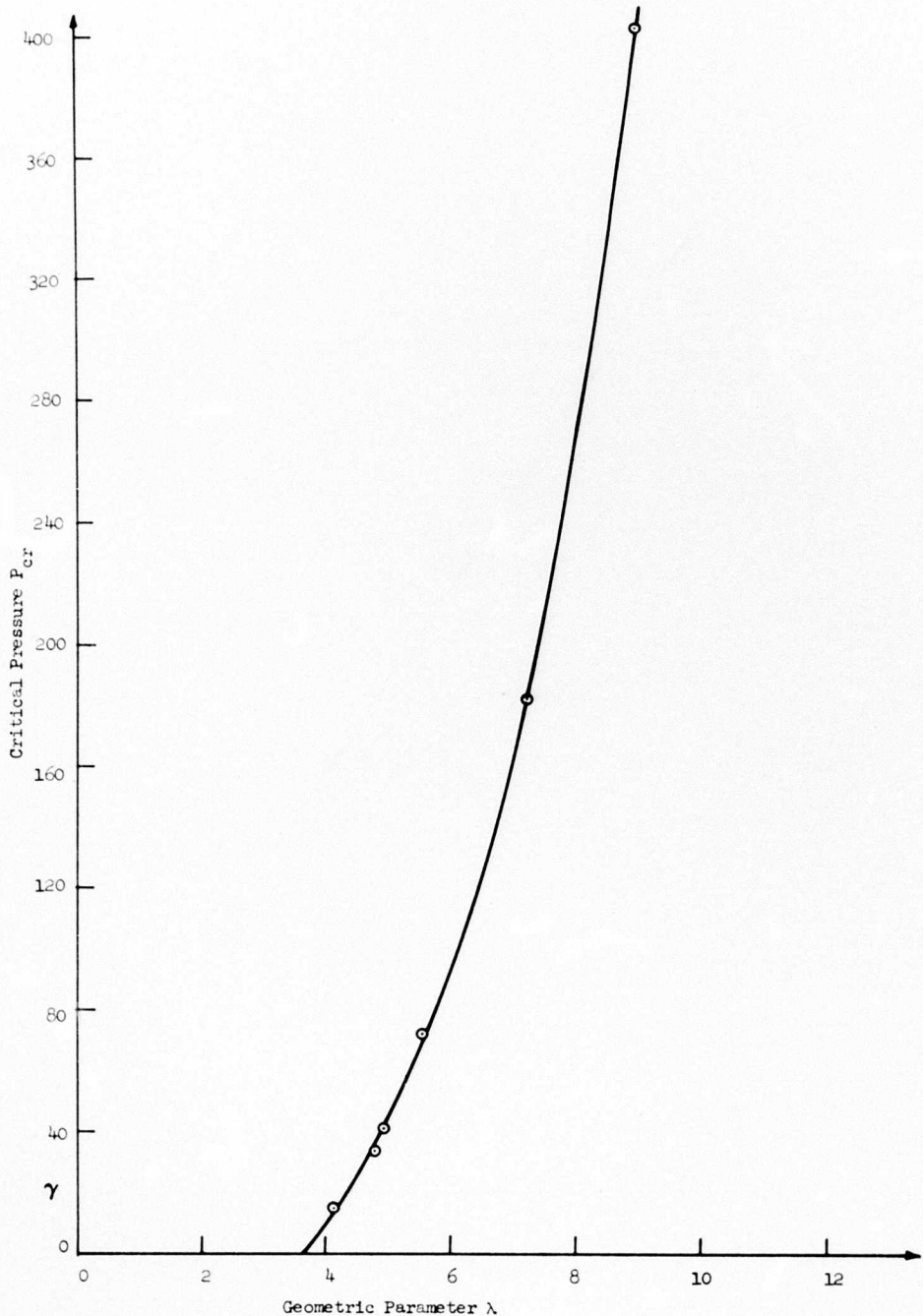


Figure 25. P_{cr} Versus λ as Derived From Southwell Plots of Kaplan and Fung's Data (Reference 21).

EXPERIMENTAL DATA OF EVAN IWANOWSKI ET AL ON SPHERICAL CAPS

From the work of Evan Iwanowski (Reference 19) on the deformation and collapse of spherical domes subjected to uniform pressure and normal concentrated loads at the apex, the three tests reported in Figure 26 have been chosen. The analyzed tests were performed on domes with clamped edges; the concentrated load at the apex was given a constant displacement.

The same procedure as before is used, and the numerical values are reported in Table VIII to XIV. Good Southwell plots result. These are presented in Figures 27, 28, and 29.

In a prior paper, Evan Iwanowski, Cheng, and Loo reported tests made on spherical caps with concentrated loads applied at the apex. In this work several of the load curves are seen to be hyperbolic in form. These have been analyzed in Figures 30 and 31. The Southwell plots which correspond to these curves are given in Figures 32, 33, 34, and 35. When the slope values from these presentations are plotted against the appropriate geometric parameter, they are seen to form a smooth curve (Figure 36).

ASHWELL'S EXPERIMENTAL DATA ON SPHERICAL CAPS

Ashwell (Reference 16) has performed four experiments on aluminum spherical caps subjected to a point load. We have selected the experiment reported in Figure 37 because, from the value of λ (geometrical parameter) equal to $\lambda = 6.4$, one obtains about the same value of P_c , according to Ashwell's and Biezeno's theories. We have shown in Table XV and in Figure 38 that a Southwell plot can be derived for this experiment, and that the slope of the straight line so obtained gives $P_c = 3.09$, a value which is in agreement with both Ashwell's and Biezeno's theories (as shown in Figure 39).

EXPERIMENTS ON A NICKEL SPHERE

The vehicle used for these tests was a complete sphere built by Sendelbeck (Reference 25). Its geometric properties were

Radius 4.2 in.
Thickness 2.1×10^{-3} in.

It was subjected to uniform external pressure, and the inward motion of the wall under this loading condition was measured with a Fotonics sensor. This device is a noncontacting optical measurement instrument. It is capable of determining motion of a reflecting surface to an accuracy of 1 micron.

The load-displacement curve obtained for the randomly chosen point was a straight line. From this line, the mechanical properties of the material, at least the Young's modulus, were computed to be as follows:

$$E = 29.3 \times 10^6 \text{ lb/in.}^2$$

This value is in excellent agreement with that determined by Carlson, Sendel-

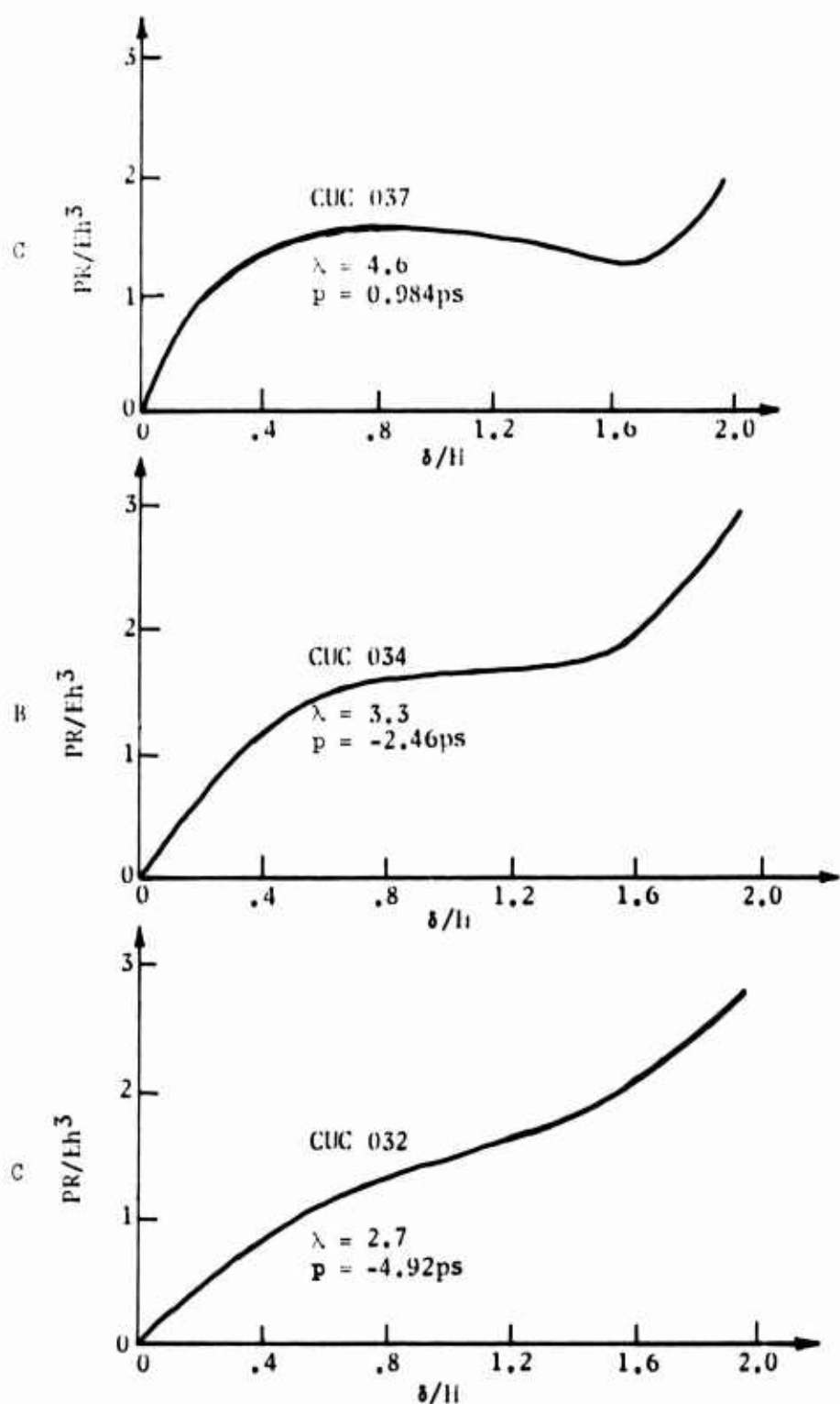


Figure 26. Load-Displacement Curves of Spherical Caps Subjected to Internal Pressure and Concentrated Load at the Apex (Loo and Evan Iwanowski, Page 303), Boundary Condition, Edges Clamped.

TABLE IX. EVAN IWANOWSKI AND LOO (CUC 03⁴, Page 303)

δ	P	δ/P
.4	1.18	.330
.5	1.33	.376
.6	1.44	.417
.7	1.53	.457
.8	1.6	.500

TABLE X. EVAN IWANOWSKI AND LOO (CUC 032, Figure 13)

δ	P	δ/P
0.5	1.02	.490
0.6	1.15	.538
0.7	1.210	.578
0.8	1.295	.617
0.9	1.38	.652
1.0	1.455	.686
1.1	1.525	.720
1.2	1.615	.760

TABLE XI. EVAN IWANOWSKI, CHENG, AND LOO (SC 303)

W	P	W/P
.9	6.62	.1355
.8	6.2	.129
.7	5.69	.123
.6	5.13	.117
.5	4.51	.1108
.4	3.81	.1052

TABLE XII. EVAN IWANOWSKI, CHENG, AND LOO
(SC 041, Figure 18)

$\lambda = 6.30$		
δ	$\frac{PR}{ER^3}$	$\frac{Eh^3}{PR}$
.2	1.53	.13
.25	1.75	.143
.3	1.86	.161
.35	1.98	.177
.4	2.08	.192
.45	2.16	.208
.5	2.24	.223
.55	2.30	.239
.6	2.35	.255
.65	2.39	.271
.7	2.42	.289
.75	2.45	.306
.8	2.46	.324

TABLE XIII. EVAN IWANOWSKI, CHENG, AND LOO
(SC 042)

$\lambda = 6.99$		
δ h	$P = \frac{PR}{Et^3}$	δ/P
.2	1.88	.100
.25	2.06	.121
.3	2.25	.133
.35	2.38	.147
.4	2.52	.159
.45	2.63	.171
.5	2.74	.183
.55	2.85	.193
.6	2.93	.205

TABLE XIV. EVAN IWANOWSKI, CHENG, AND LOO

δ/h	$\frac{PR}{Et^3}$	Corrected	
.2	1.59	.73	.274
.25	1.85	.81.8	.295
.3	2.12	.974	.308
.35	2.31	1.050	.333
.4	2.45	1.12	.357
.45	2.59	1.19	.378
.5	2.70	1.24	.403
.55	2.78	1.275	.432

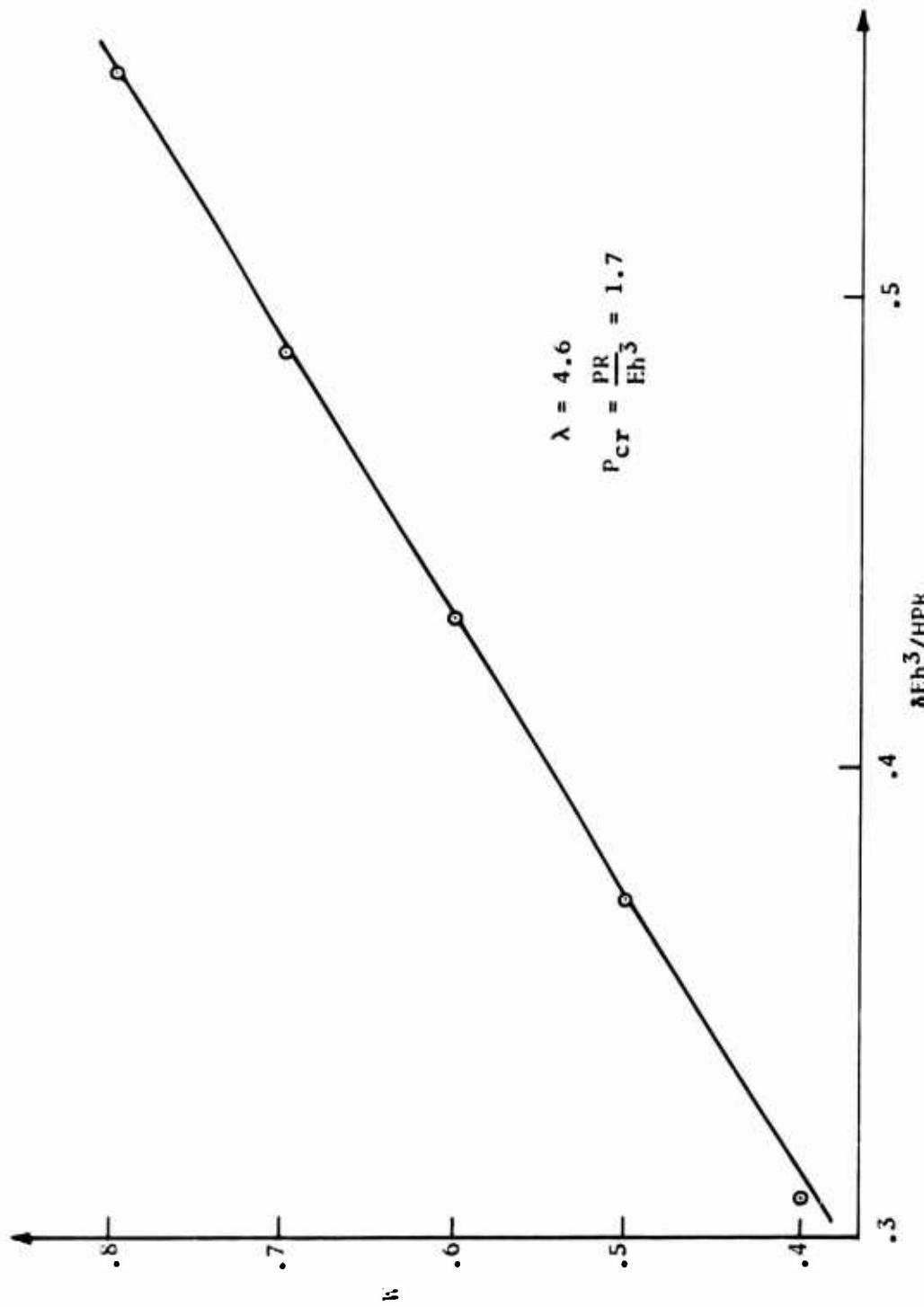


Figure 27. Southwell Plot of Specimen CUC 037 (Loo and Evan Iwanowski).

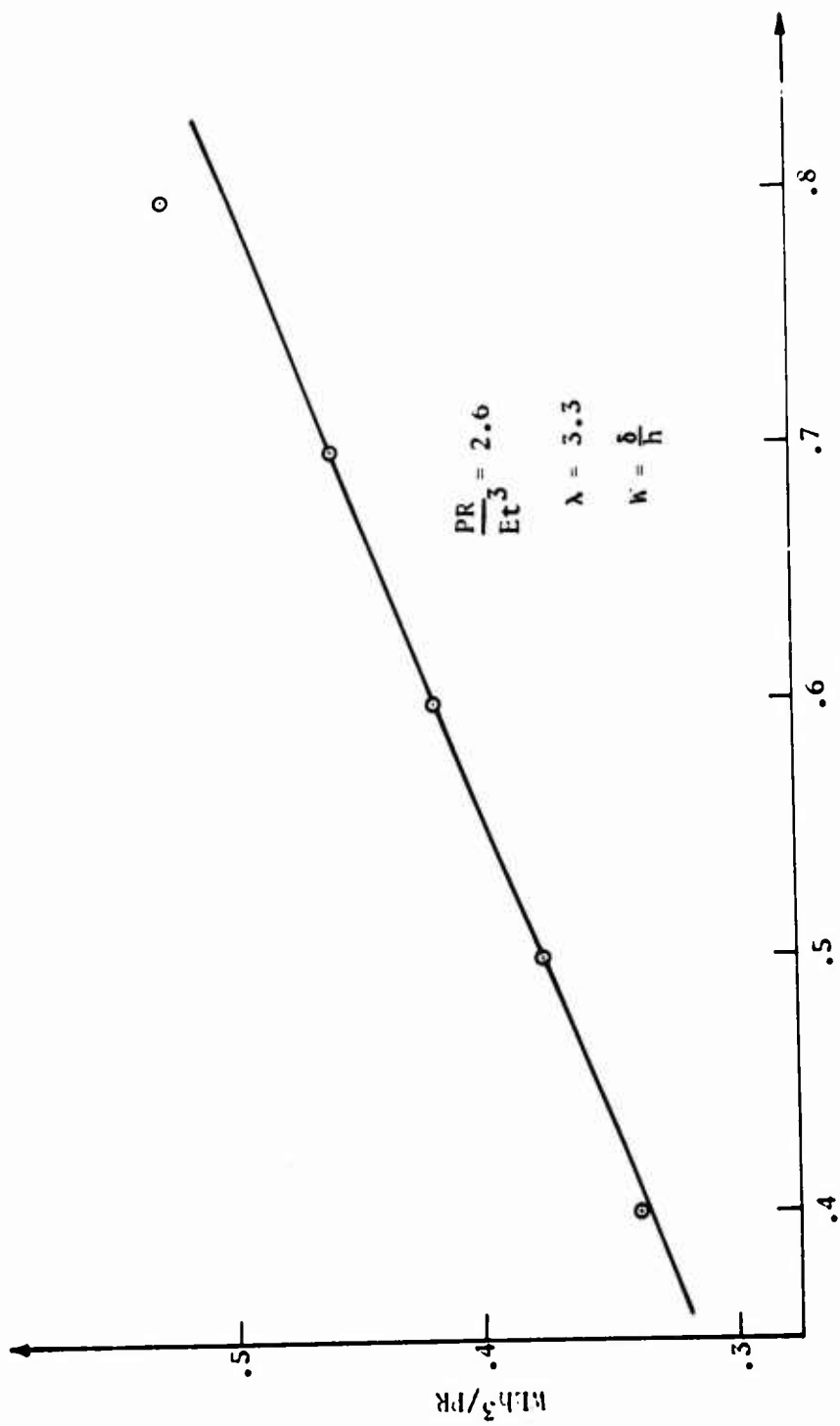


Figure 28. Southwell Plot of Specimen CUC 034 (Loo and Ivan Iwanowski).

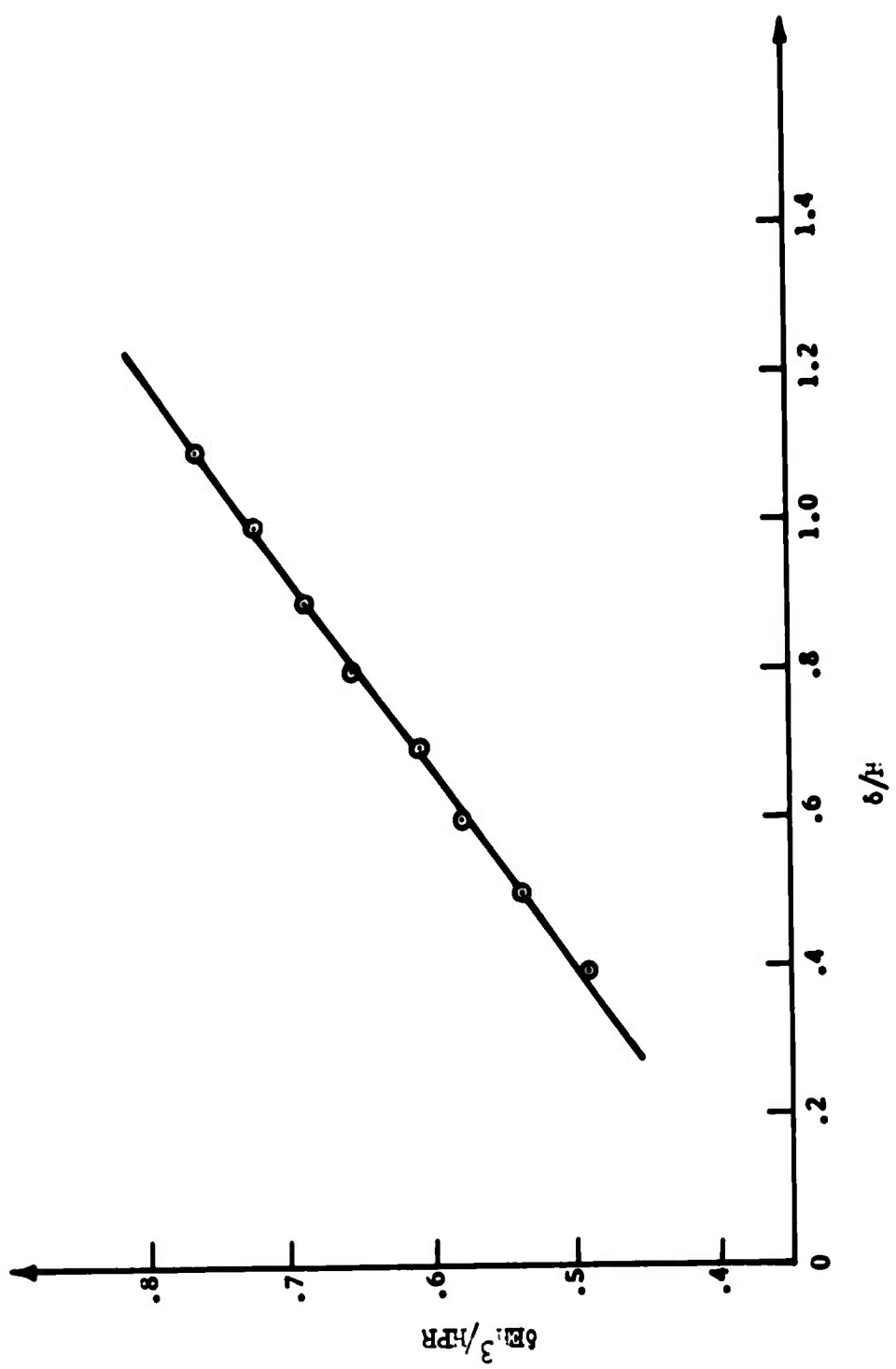


Figure 29. Southwell Plot of Spherical Dose Subjected to Uniform Pressure and Normal Concentrated Load at the Apex (Specimen CUC 032 - Loo and Evan Ivancsik).

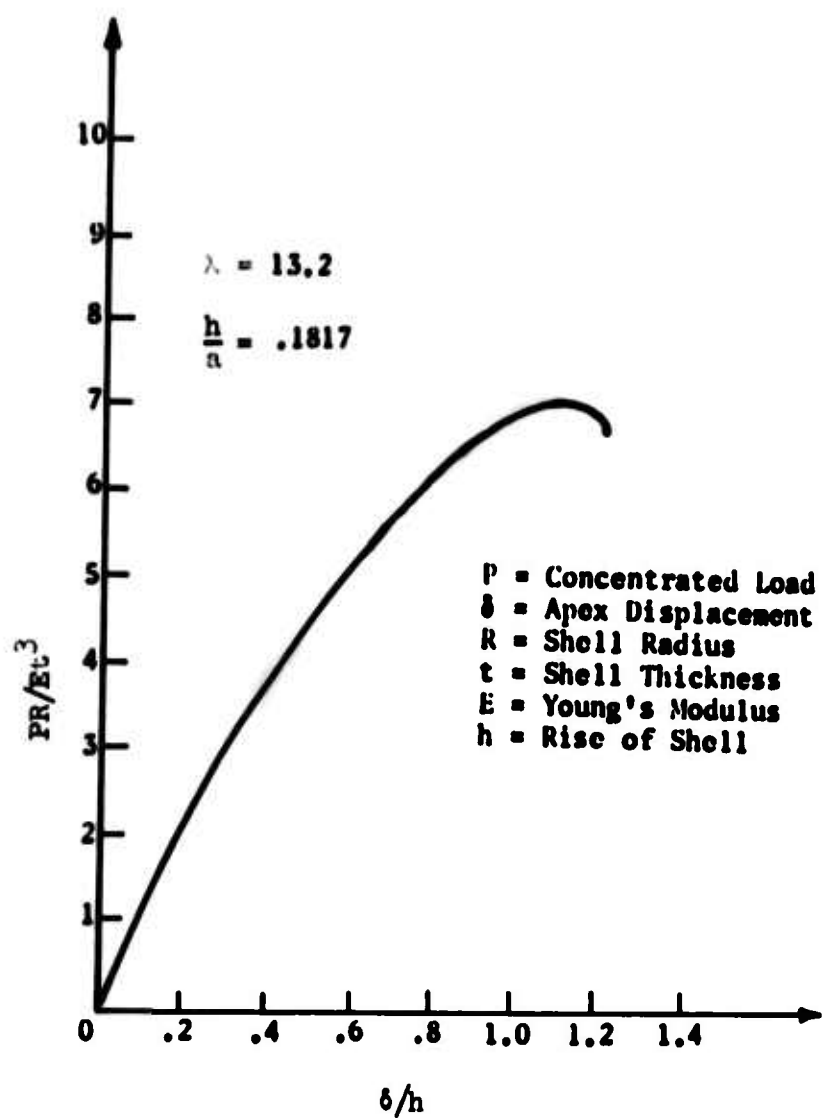


Figure 30. Symmetric Mode of Buckling (Evan Iwanowski, Cheng, and Loo, Figure 1A, Page 572) SC 303.

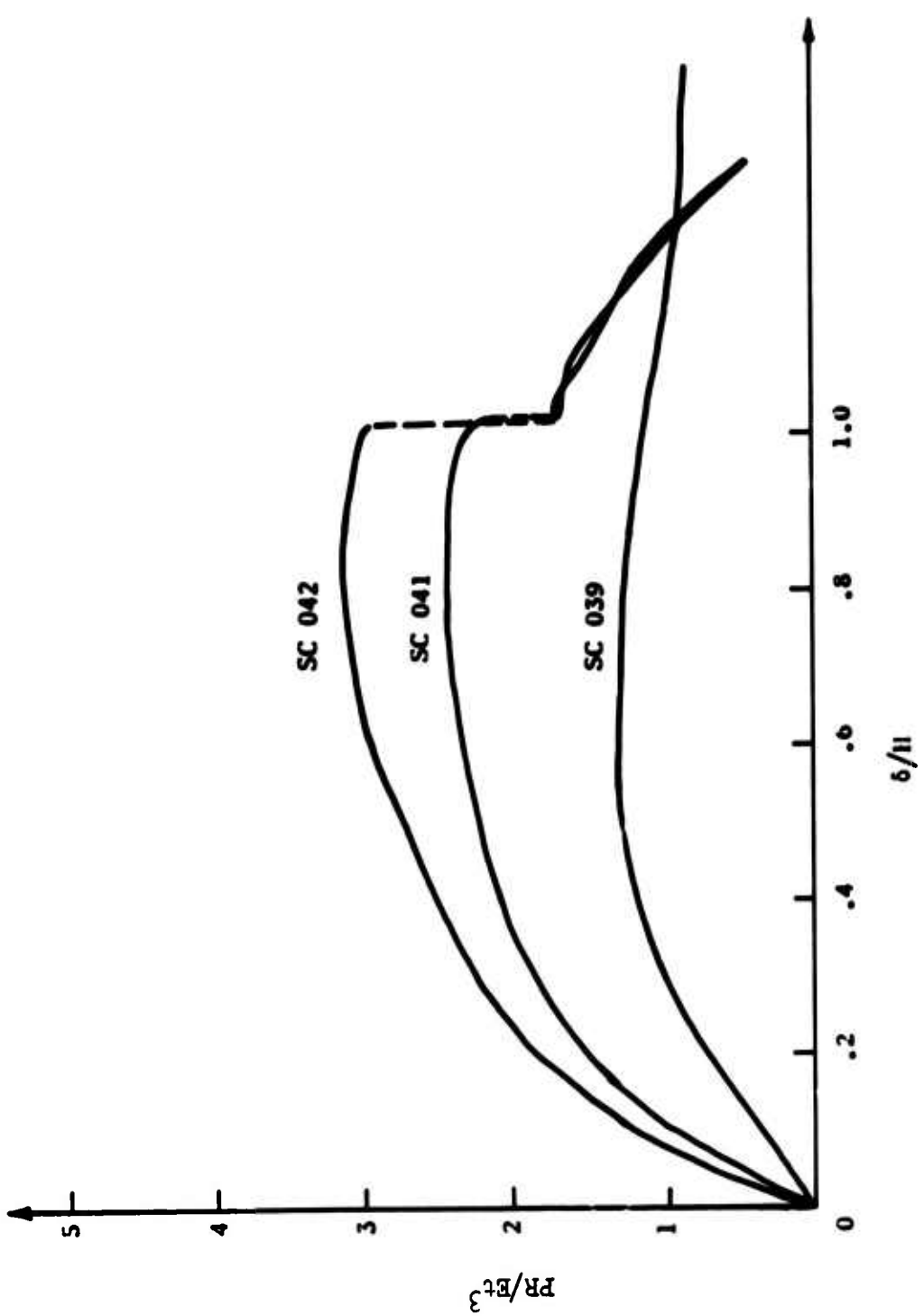


Figure 31. Load-Deflection Curves of a Spherical Dome Subjected to a Concentrated Load at the Apex (Evan Iwanowski, Cheng, and Loo).

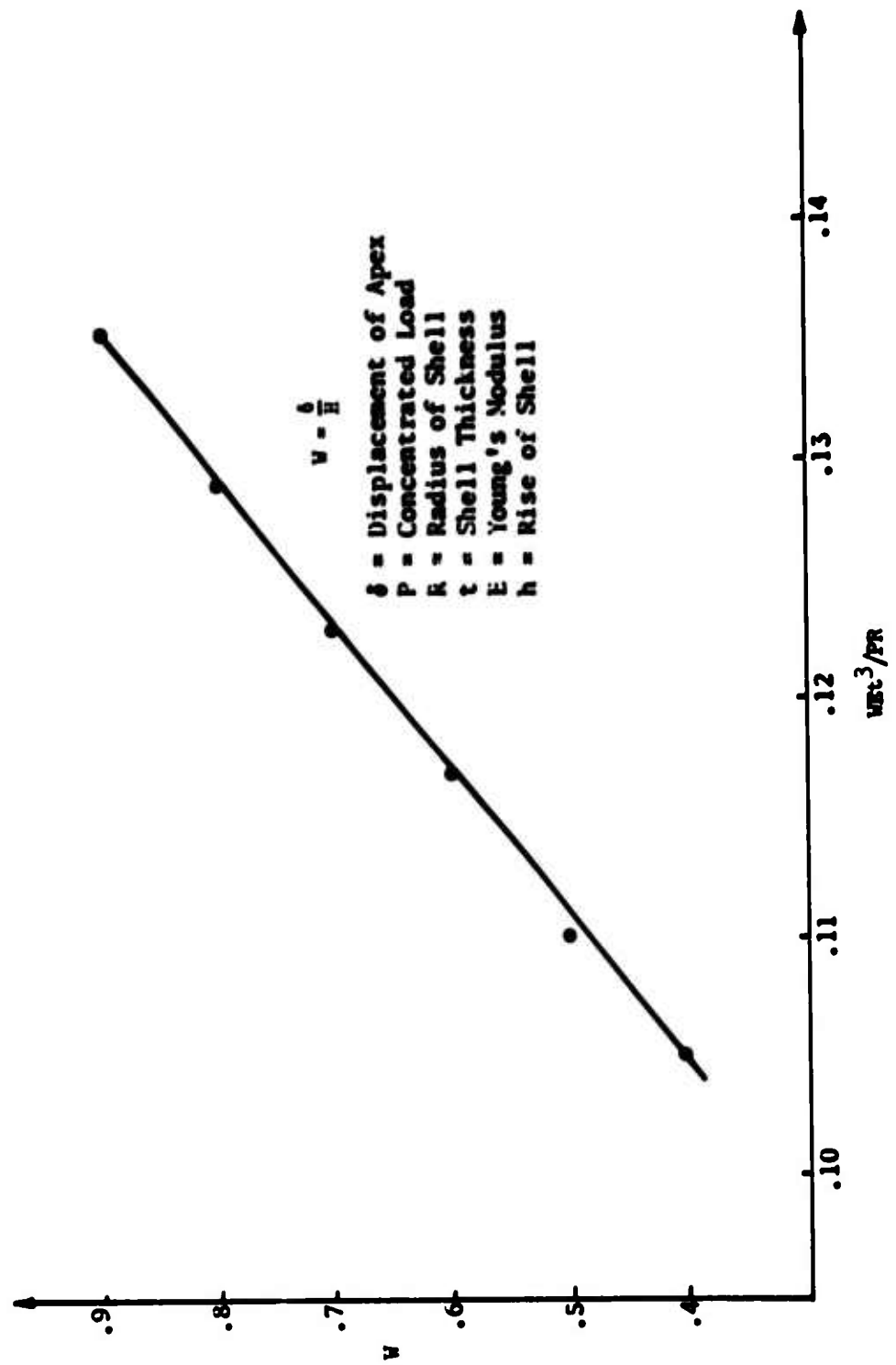


Figure 32. Loo, Cheng, and Evan Iwanowski Data on Spherical Cap Subjected to Concentrated Load at the Apex (Figure 14, SC 303).

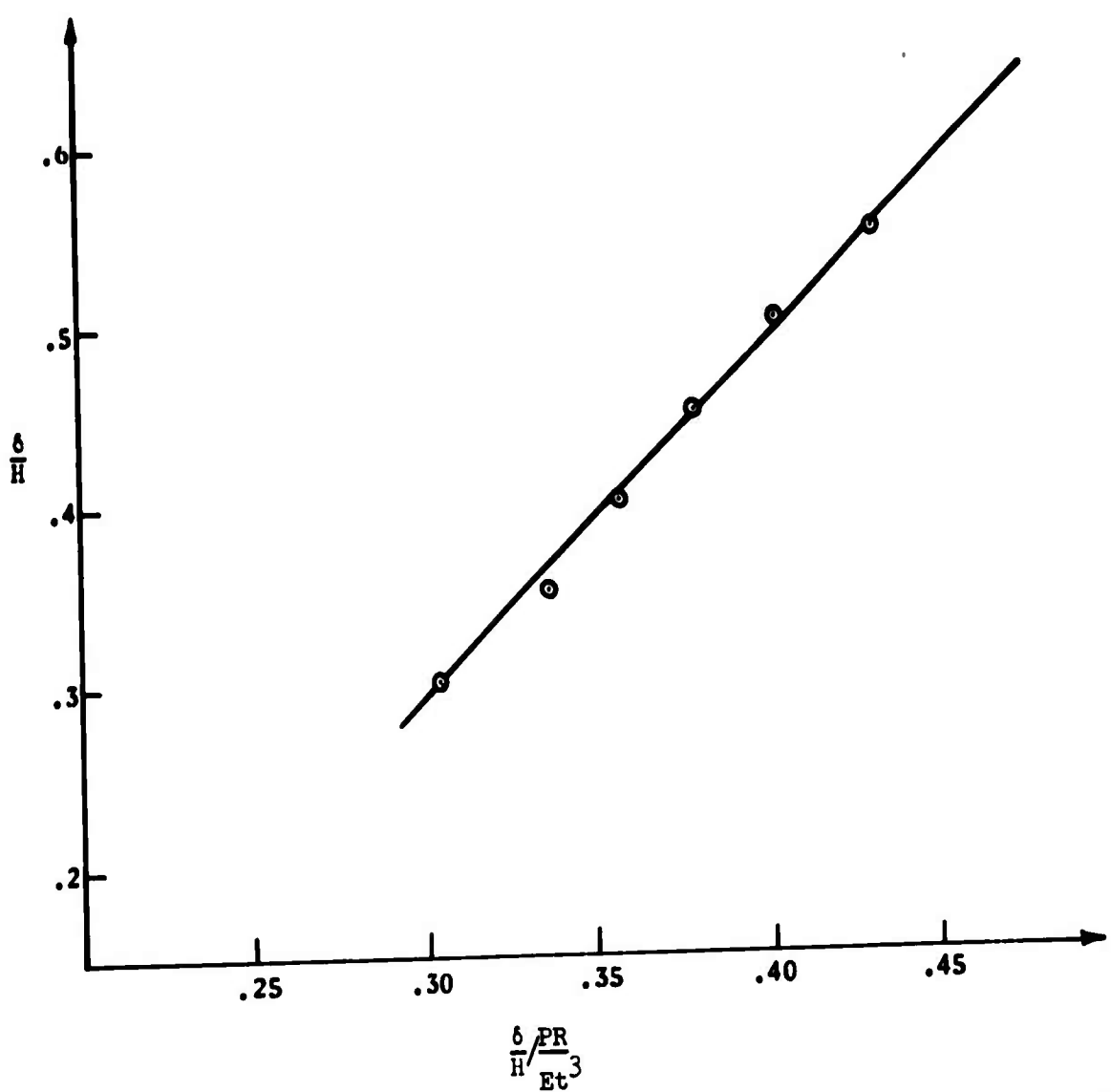


Figure 33. Southwell Plot of Specimen SC 039 (Loo, Cheng, and Iwanowski).

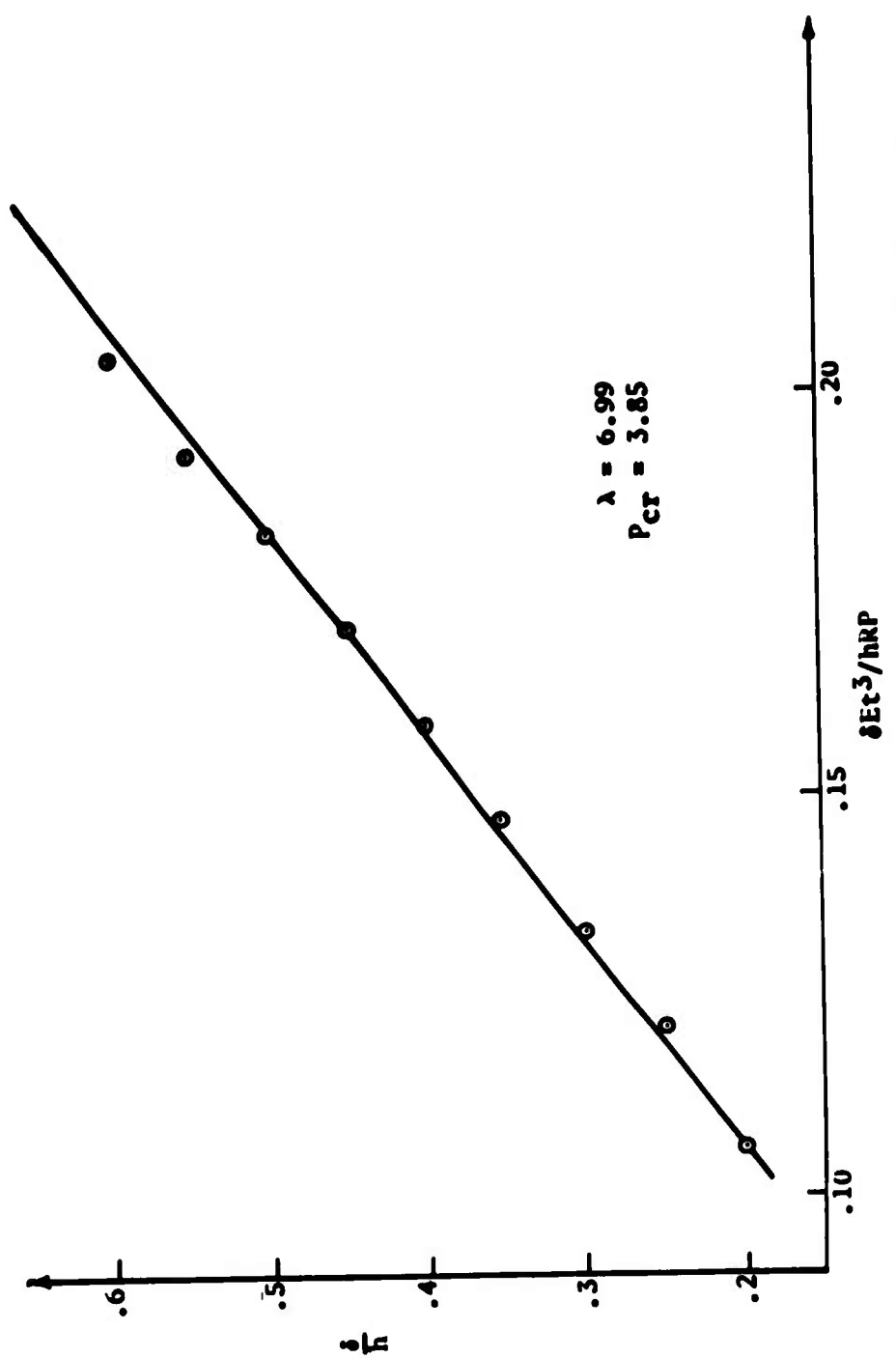


Figure 34. Southwell Plot of Specimen SC 042 (Loo, Cheng, and Ivanouski).

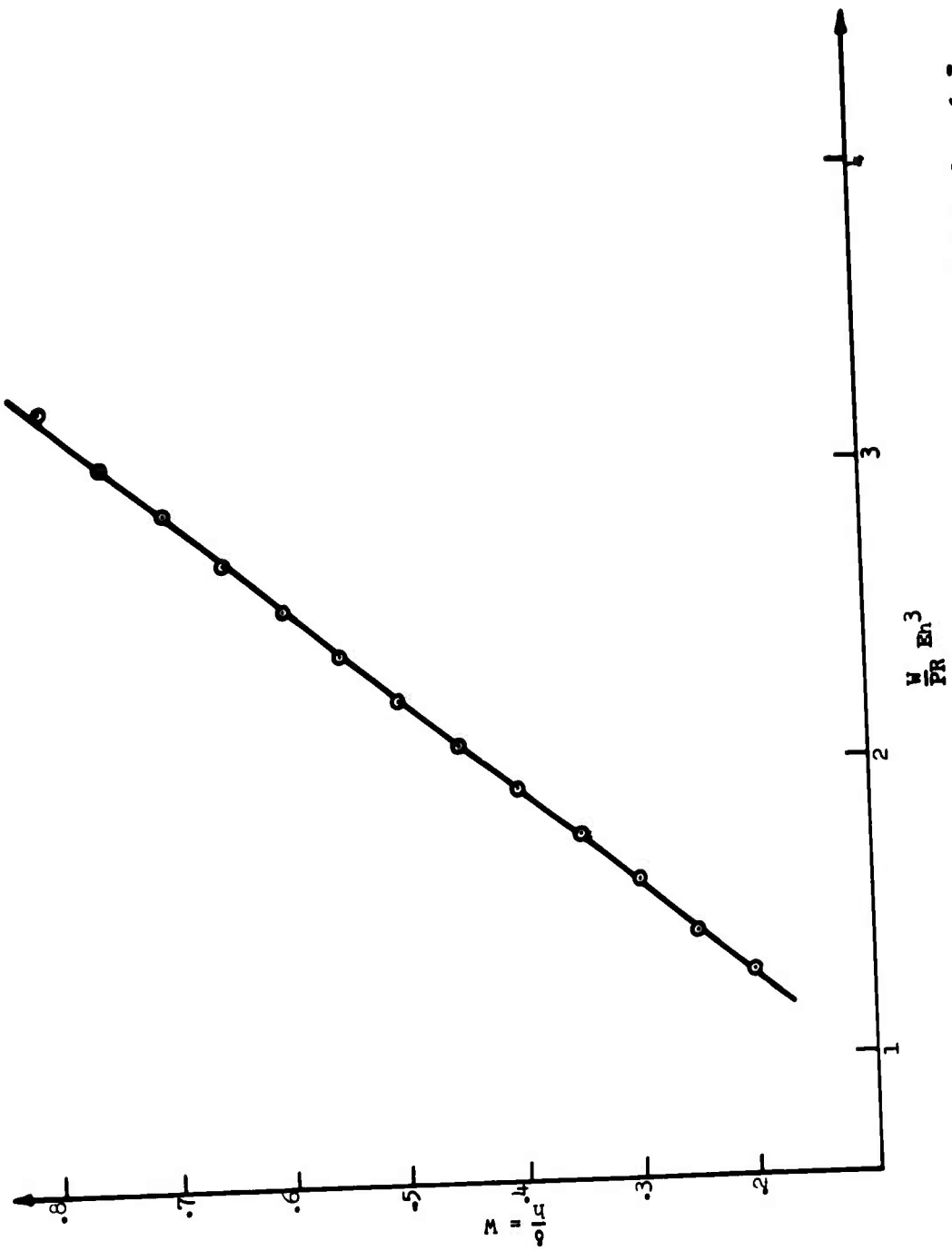


Figure 35. Loo, Cheng, and Iwanowski's Data on Spherical Cap - SC 041, $\lambda = 6.3$.

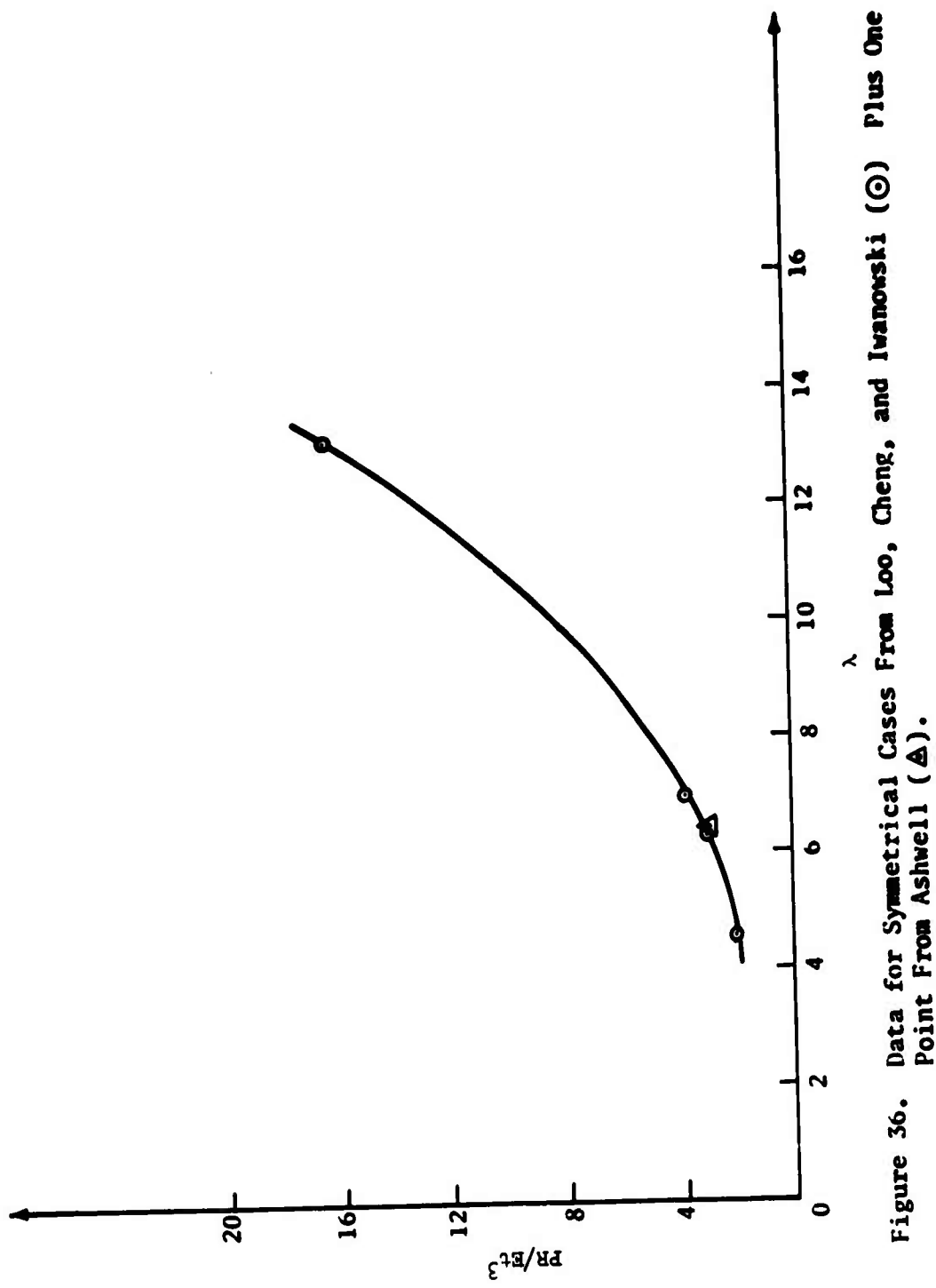


Figure 36. Data for Symmetrical Cases From Loo, Cheng, and Ivanovski (○) Plus One Point From Ashwell (Δ).

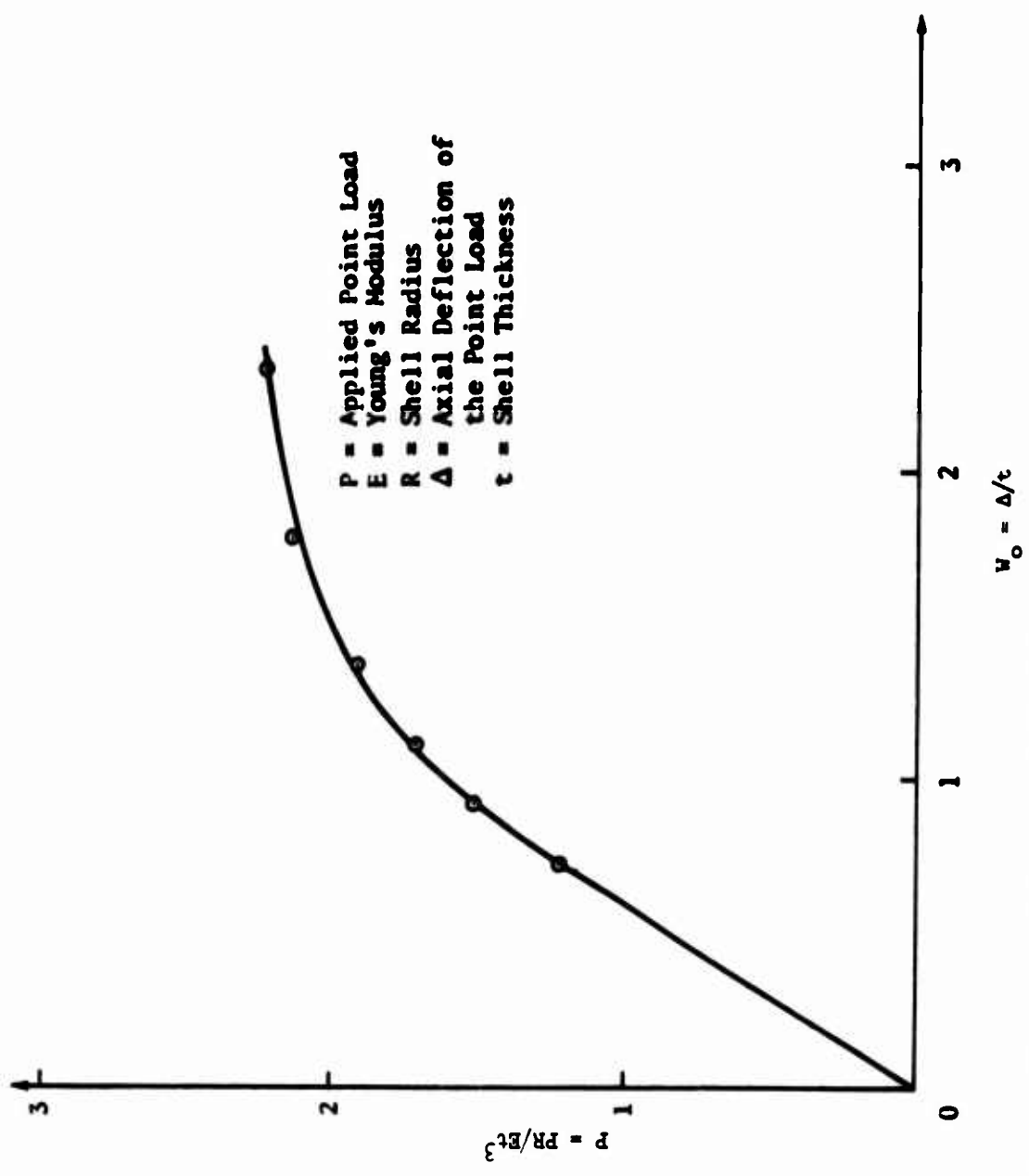


Figure 37. Ashwell's Experimental Data for a Sphere with Point Load at the Apex.

TABLE XV. ASHWELL (Reference 16, Figure 12, Page 60)

$a^t = 6.4$		
w_o	P	w_o/P
2.33	2.23	1.04
1.8	2.13	.845
1.38	1.9	.727
1.11	1.7	.655
.93	1.51	.555
.737	1.21	.535

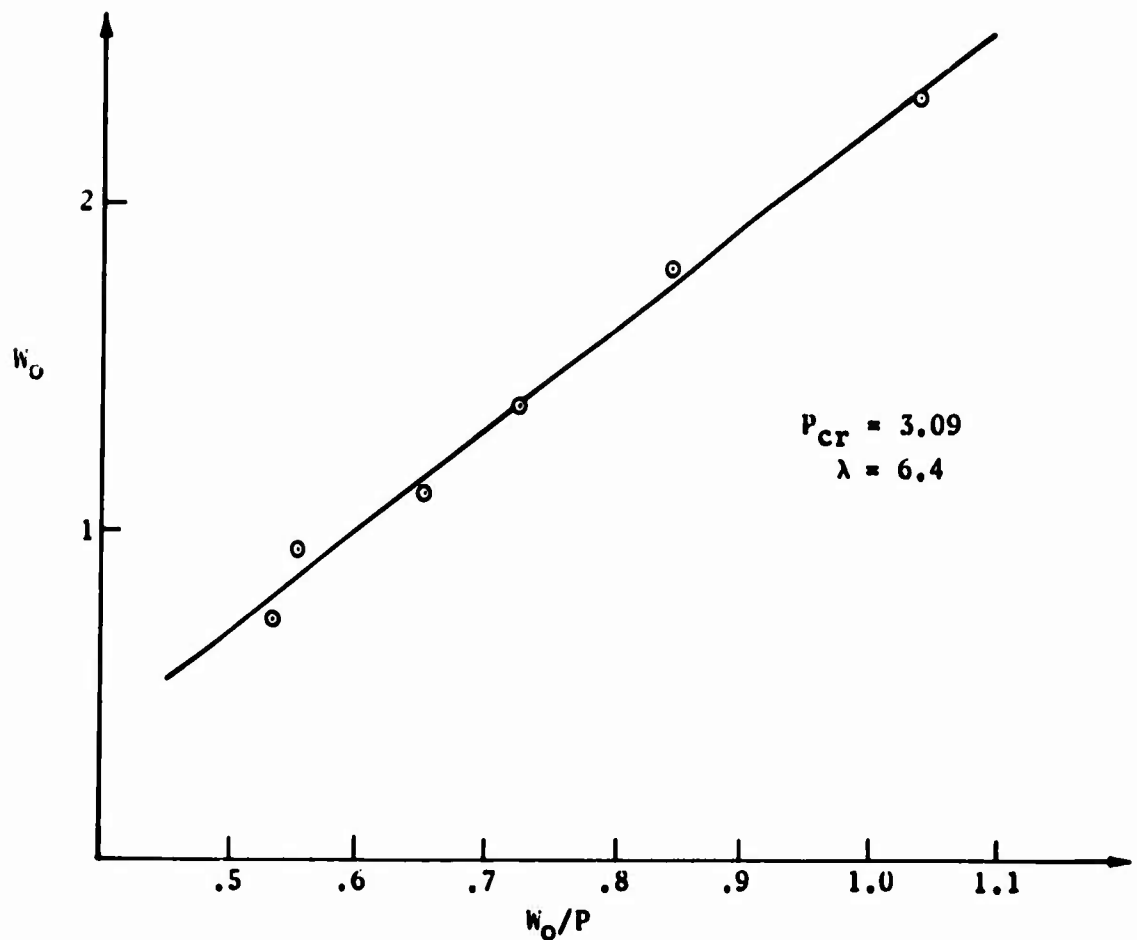


Figure 38. Ashwell's Experimental Data.

○ Results Obtained From
Ashwell's Experiment
Through the Southwell
Analysis

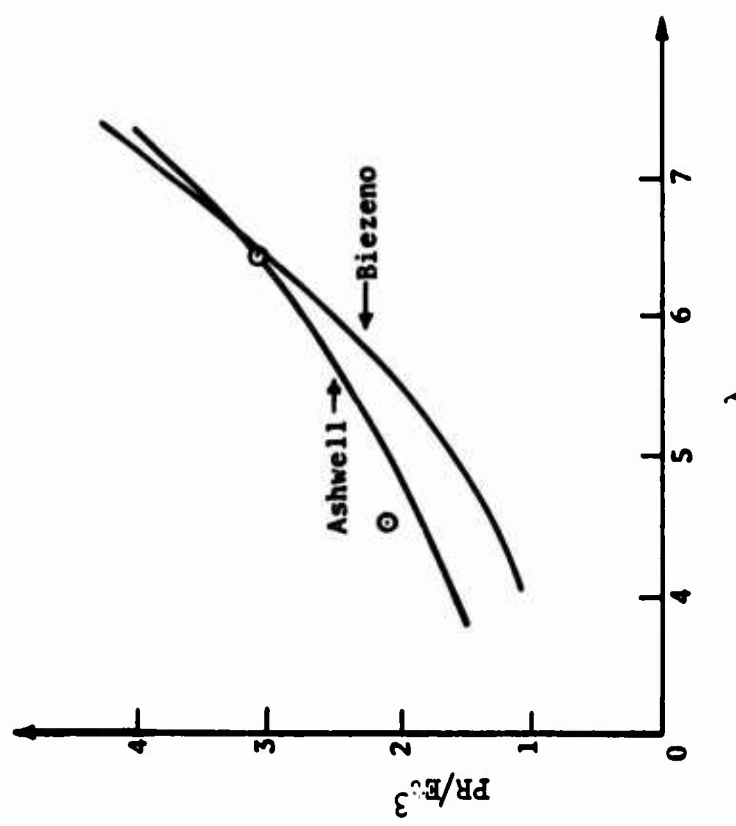


Figure 39. Theoretical Curves of the Critical Load of a Spherical Cap Subjected to a Concentrated Load Versus λ (Geometrical Parameter).

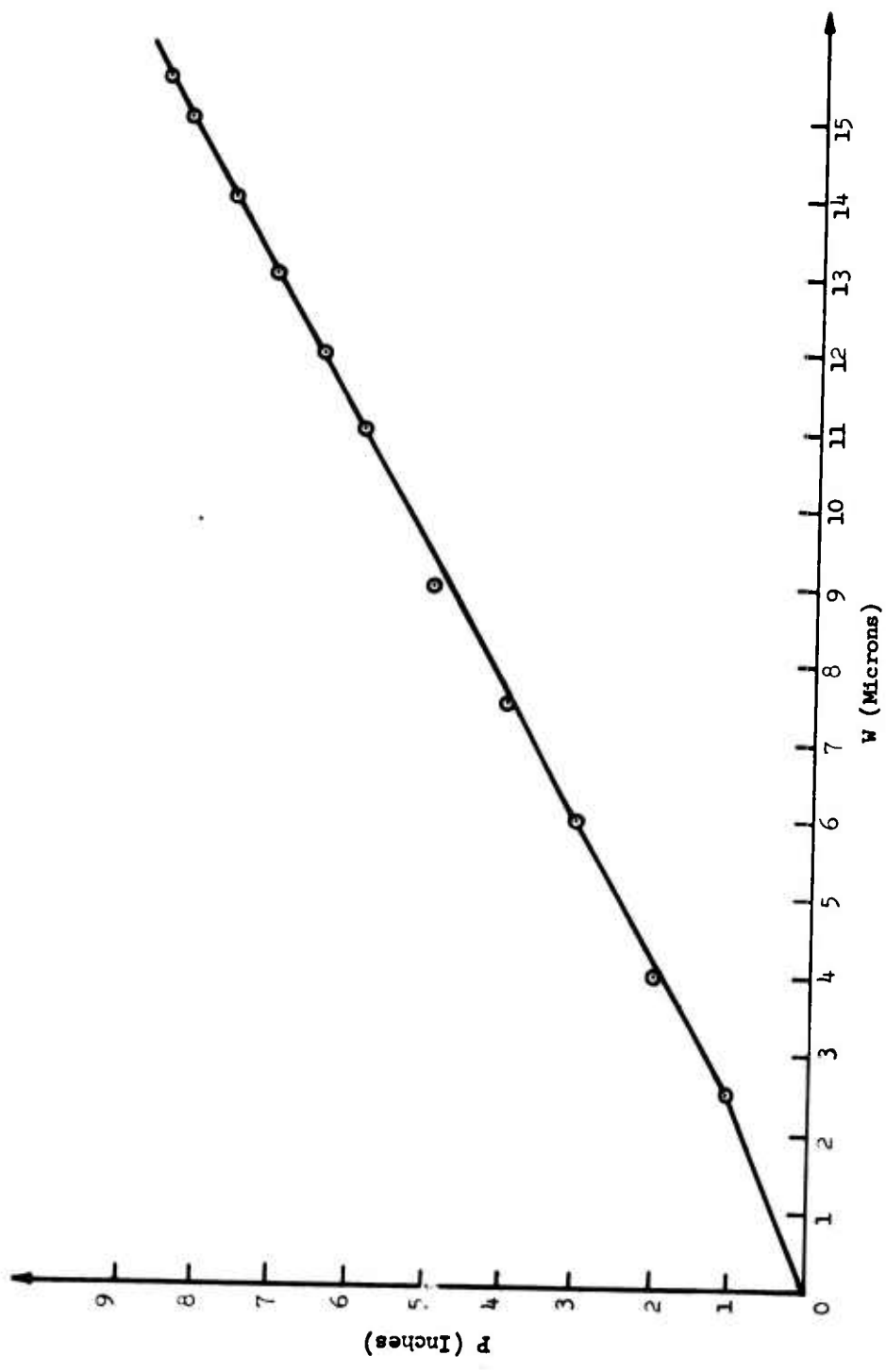


Figure 40. Radial Displacement Versus External Pressure for Nickel Sphere S958,
Test I.

TABLE XVI. TEST I - SPHERE - S958

P (in.Hg)	W (microns)
1	2.5
2	4
3	6
4	7.5
5	9
5.9	11
6.45	12
7.05	13
7.65	14
8.25	15
8.55	15.5

Determination of E From Figure 38	
$E = \frac{6}{\epsilon} = \frac{R}{w} \frac{pR}{2t}$	w = 10 microns
	p = 5.8 in.Hg
$E = 29.3 \cdot 10^6$	lb/sq in.

beck, and Hoff (Reference 12) from similar vehicles. The value of Poisson's ratio was taken to be 0.3.

With these geometric and mechanical properties, the shell had a theoretical critical pressure given by

$$P_{cr} = 2 \times 0.6 \times 29.3 \times 10^6 \times \left(\frac{2.1}{4.2}\right)^2 \cdot \frac{1}{10^6} \text{ psi}$$

$$= 0.3 \times 29.3 \text{ psi} = 8.79 \text{ psi}$$

During the first test on the vehicle, the point of first buckling was determined. The motion permitted during this test was very slight; and as a consequence, the sphere was not damaged by the test. The Fotonics sensor was repositioned at the center of the prime buckle, and the test was repeated. The load displacement was recorded and is as depicted in Figure 41. It is seen from this figure that initially the sphere has a linear relationship between load and displacement, but there comes a point at which the character of this motion changes. The displacement curve appears to be hyperbolic.

When the hyperbolic portion of the curve is examined from the Southwell linear relationship aspect, it is seen (Figure 42) that a very good straight line exists. The slope of this line is computed to be 3.93 psi, a value which should agree with the classic critical value. There is a most unfortunate discrepancy; the ratio of

$$\frac{\text{critical}}{\text{classical}} \text{ is } \frac{3.93}{8.79} = .447$$

It is seen in Figure 41 that the initial portion of the load-displacement curve is linear. When a modulus value for the sphere is computed from this, the local modulus is much less than that previously determined. In fact, the ratio of this modulus to the quoted value is

$$\frac{290}{585} = .496$$

Hence, we conclude that in this case at least we have established that the cause of the discrepancy lies in a local reduction in effective modulus. The correlated ratio of determined critical pressure to classic value is .92.

However, it is important to realize that the local correction for modulus could not have been observed if extremely sensitive transducers had not been used. The overall displacement used in the computation is of the order of 7 microns.

EXPERIMENTS ON A PLASTIC SPHERE

Thompson (Reference 18) reported what is probably the first load-displacement

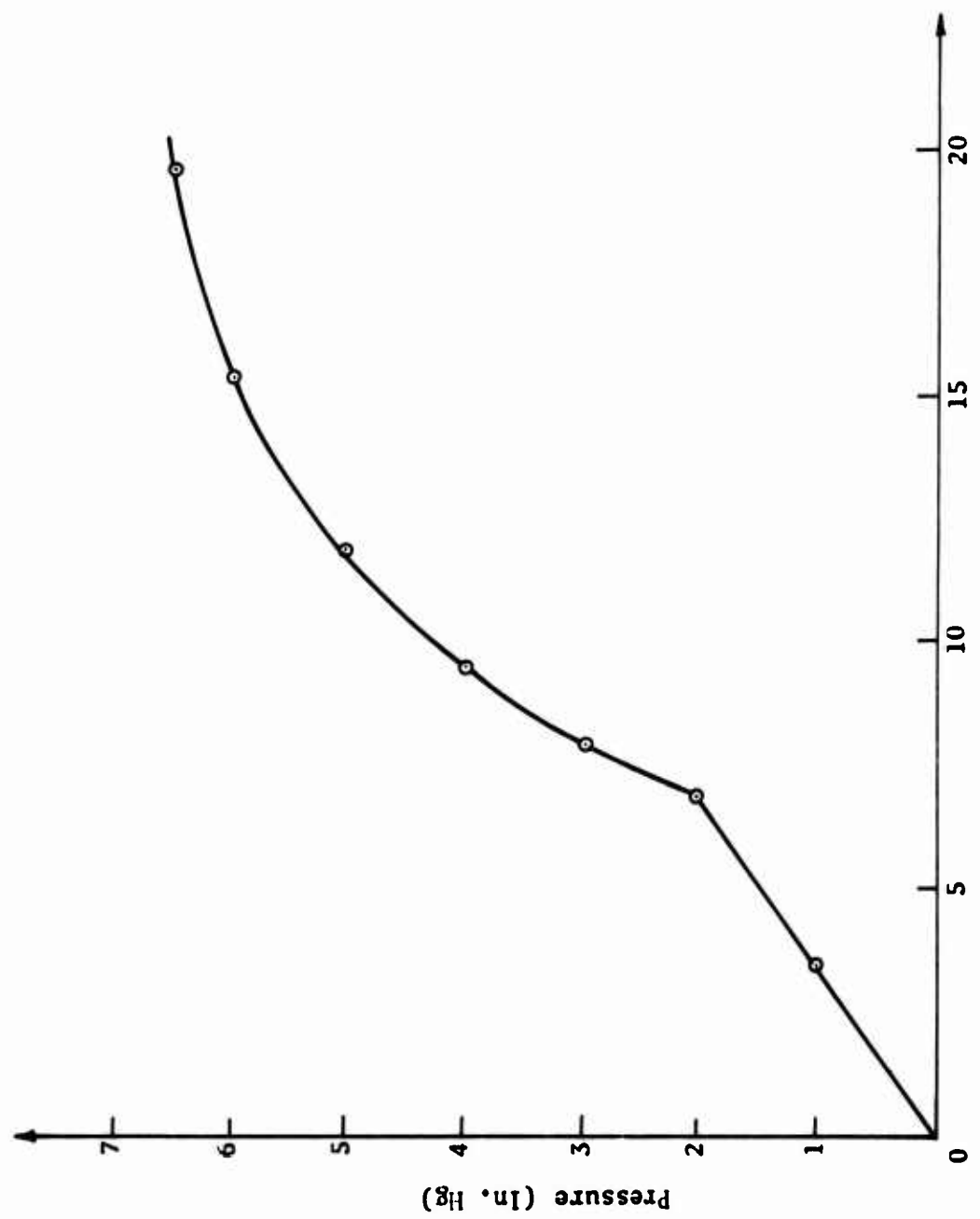


Figure 41. Pressure-Displacement Relationship for Nickel Sphere S958, Location 1,
Run 1, Test II.

TABLE XVII. TEST II SPHERE S958

P (in. Hg)	W (microns)	$w - w_o / P^*$
0	0	
1	3	
2	7	4.00
3	8	5.33
4	9.5	7
5	12	9.4
6	15.5	12.66
6.5	19.75	16.8

*The abscissa is taken for $w_o = 6$ microns.

$w - w_o$ is measured in mm. in Figure 41 from this new origin.

TABLE XVIII. THOMPSON DATA

w	P/P_c^*	$w/P/P_c$
.74	2.75	.261
.85	2.97	.279
.9	3.14	.287
1.08	3.4	.312
1.27	3.66	.345
1.4	3.78	.37
1.62	3.83	.423

*A scale factor of .2/1.68 takes care of the units chosen in the present table. Computation of E

$$E = \frac{6}{\epsilon} = \frac{R}{m} \quad \frac{pR}{2t} = \frac{pR^2}{2wt^2} \frac{\sqrt{3(1-\mu^2)}}{1-\mu}$$

$\mu = .48 \quad t = .1 \quad R = 2.1 \quad E_{th} = 450$

$P/P_c = .6 \quad w = 1.41 \quad E = 348$

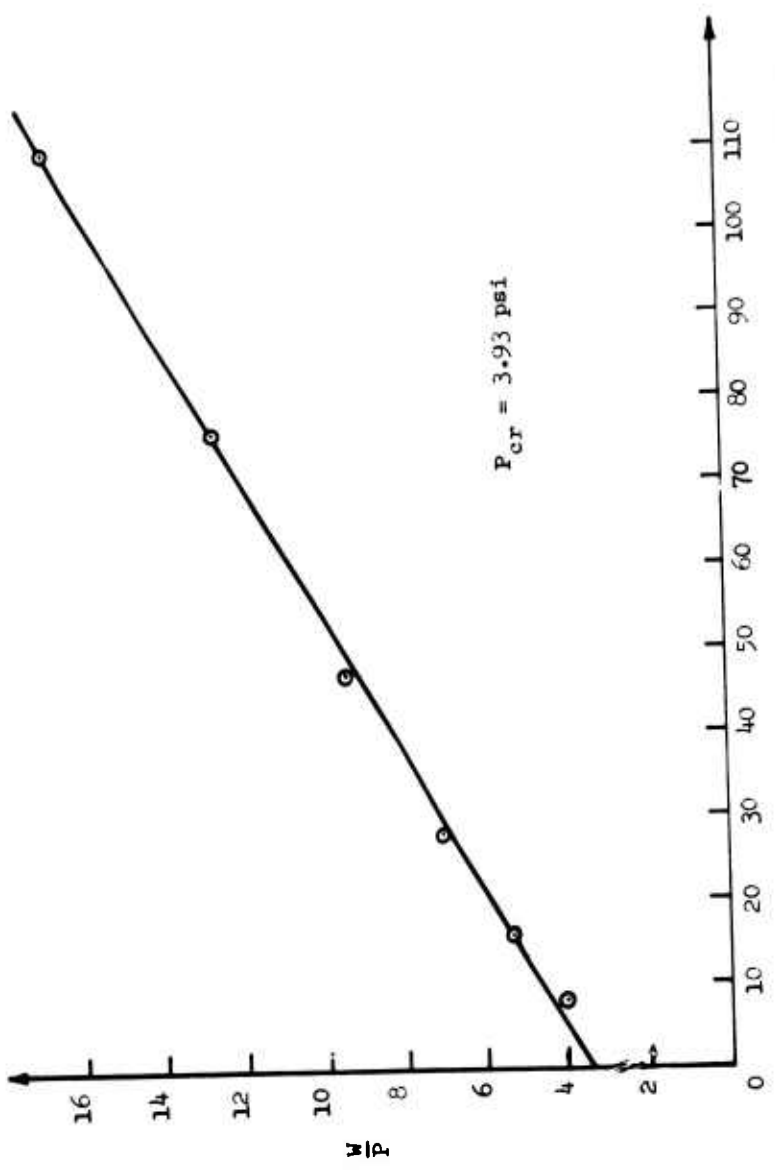


Figure 42. Southwell Plot for the Data of Tests on Sphere S958, Location 1,
Run 1, Test 11.

study on a complete spherical shell. The data which he gave are reproduced in Figure 43. If these data are examined in the manner previously discussed, then the relationship between the elastic deformation and the pressure which produces it is as given in Table XIX. When these results are plotted (Figure 44), it is seen that the Southwell linear relationship exists and that the value of the critical pressure derived from this plot ($P/P_{cr} = .774$) does not agree with the theoretical level ($P/P_{cr} = 1$), when this level is computed on the basis of natural properties given by Thompson. However, if the sphere modulus is determined from the natural slope of the load-displacement curve, it is found that Thompson's value of modulus is in error. The effective modulus is less than he prescribed. From the curve which he shows, the modulus is 396 psi, whereas the computation of P/P_{cr} was made on the basis of 450 psi. The slope of the Southwell line is computed to be $P/P_{cr} = .999$. Thus, when this is corrected by the ratio of 450/396 which takes into account the local E variation, we find that the classic critical value is established.

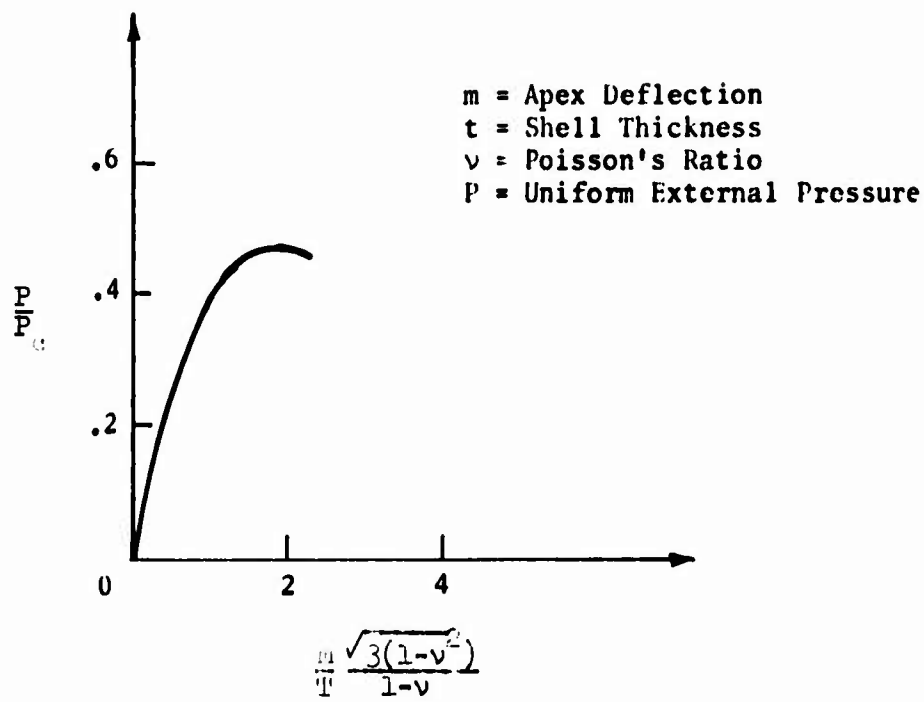


Figure 43. Dimple Amplitude Parameter Versus Pressure
 (Reference Thompson, Figure 5, Page 193).

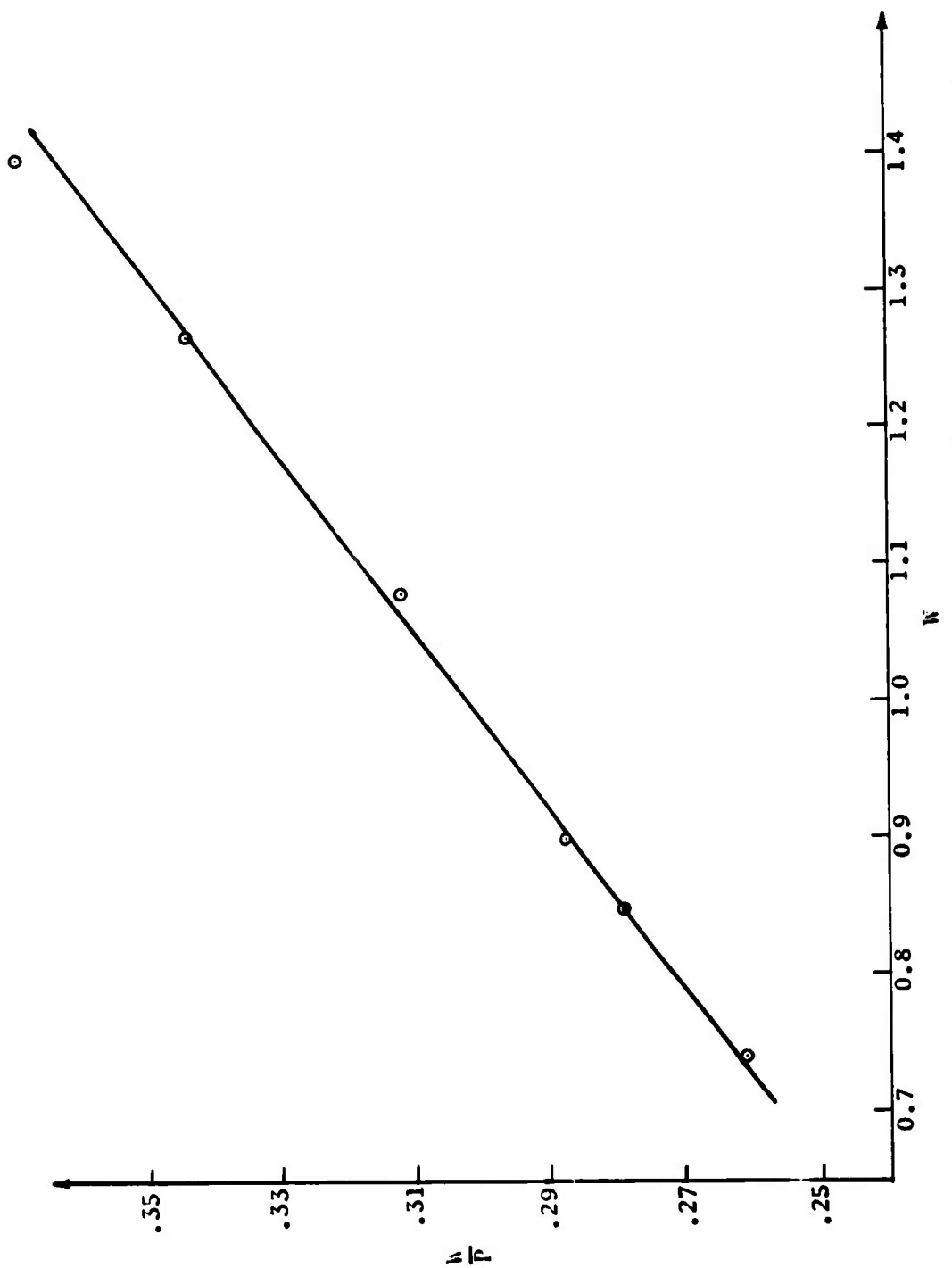


Figure 44. Southwell Plot for Thompson's Experimental Data on a Sphere Under External Pressure (Reference 29).

REFERENCES

1. Westergaard, H. M., BUCKLING OF ELASTIC STRUCTURES, Transactions of American Society of Civil Engineers, Vol. 85, 1922, pp. 576-654.
2. Southwell, R. V., ON THE ANALYSIS OF EXPERIMENTAL OBSERVATION IN PROBLEMS OF ELASTIC STABILITY, Proceedings of the Royal Society, Vol. 135A, 1932, p. 601.
3. Zoelley, R., ÜBER EIN KNICKUNGSPROBLEM AN DER KUGELSCALE, Diss. Zurich, 1915.
4. Schwerin, E., ZUR STABILITAT DER DUNWANDIGEN HOHLKUGEL UNTER GLEICHMU^BGIGEM AUBENDRUCK, Zeitschrift fur Angewandte Mathematik und Mechanik, Vol. 2, 1922, pp. 81-91.
5. Van der Neut, A., THE ELASTIC STABILITY OF THE THIN-WALLED SPHERE (in Dutch), Diss. Delft, 1932.
6. Biezeno, C. B., ÜBER DIE BESTIMMUNG DER DURCHSCHLUGKRAFT EINER SCHWACH GEKRUMMTER KREISFORMIGEN PLATTE, Zeitschrift fur Angewandte Mathematik und Mechanik, Vol. 15, 1938, pp. 13-30.
7. von Kármán, Theodore, and Tsien, Hsue Shen, THE BUCKLING OF SPHERICAL SHELLS BY EXTERNAL PRESSURE, Journal of the Aeronautical Sciences, Vol. 7, December 1939, p. 43.
8. Sechler, E. E., and Bollay, See Reference 7 above.
9. Friedrichs, K. O., ON THE MINIMUM BUCKLING LOAD FOR SPHERICAL SHELLS, Applied Mechanics, Theodore von Kármán Anniversary Volume, 1941, p. 258.
10. Tsien, Hsu Shen, A THEORY FOR BUCKLING OF THIN SHELLS, Journal of the Aeronautical Sciences, Vol. 9, No. 10, 1942.
11. Krenske, M. A., TESTS ON MACHINED DEEP SPHERICAL SHELLS UNDER EXTERNAL HYDROSTATIC PRESSURE, Report 1601, Structural Mechanics Laboratory of California Institute of Technology, May 1962.
12. Carlson, R. L., Sendelbeck, R. L., and Hoff, N. J., AN EXPERIMENTAL STUDY OF THE BUCKLING OF COMPLETE SPHERICAL SHELLS, Stanford University Report, SUDAAR 254, December 1965.
13. Kaplan, A., and Fung, Y. C., A NON-LINEAR THEORY OF BENDING AND BUCKLING OF THIN ELASTIC SHALLOW SPHERICAL SHELLS, NACA TN 3212, August 1954.
14. Horton, W. H., and Bailey, S. C., THE INFLUENCE OF TEST MACHINE RIGIDITY ON THE BUCKLING LOAD OF SHELLS, a paper presented at the American Society of Testing Materials Annual Meeting, Paper 204, Atlantic City, New Jersey, June 1966, pp. 183-213.
15. Hoff, N. J., and Soong, T. C., LOWER BOUNDS FOR THE BUCKLING PRESSURE OF SPHERICAL SHELLS, Stanford University Department of Aeronautics and

Astronautics, SUDAER 133, 1962.

16. Ashwell, D. G., ON LARGE DEFLECTION OF A SPHERICAL SHELL WITH AN INWARD POINT LOAD, Proceedings of the Symposium on the Theory of Thin Elastic Shells, edited by Koiter, Delft, 1960, p. 43.
17. Fung, Y. C., and Sechler, E. E., INSTABILITY OF THIN ELASTIC SHELLS, Structural Mechanics, Proceedings of the First Symposium on Naval Structural Mechanics, edited by J. N. Goodier and N. J. Hoff, Pergamon Press, Great Britain, 1960, p. 115.
18. Thompson, J. M. T., THE ELASTIC INSTABILITY OF A COMPLETE SPHERICAL SHELL, The Aeroneautical Quarterly, Vol. 13, Part 2, May 1962, p. 189.
19. Loo, T. C., and Evan Iwanowski, R. M., DEFORMATIONS AND COLLAPSE OF SPHERICAL CONES SUBJECTED TO UNIFORM PRESSURE AND NORMAL CONCENTRATED LOADS AT THE APEX, Proceedings of the World Conference on Shells and Structures, San Francisco, 1962.
20. Evan Iwanowski, R. M., Cheng, H. S., and Loo, T. C., EXPERIMENTAL INVESTIGATIONS OF DEFORMATIONS AND STABILITY OF SPHERICAL SHELLS SUBJECTED TO CONCENTRATED LOAD AT THE APEX, Proceedings of the Fourth U. S. National Congress of Applied Mechanics, 1962, p. 563.
21. Norton, W. H., and Durham, S. C., IMPERFECTIONS, A MAIN CONTRIBUTOR TO SCATTER IN EXPERIMENTAL VALUES OF BUCKLING LOAD, International Journal of Solids and Structures, Vol. 1, Pergamon Press, 1965, pp. 59-74.
22. Horton, W. H., Cundari, F. L., and Johnson, R., ON THE APPLICABILITY OF THE SOUTHWELL PLOT TO THE INTERPRETATION OF TEST DATA OBTAINED FROM INSTABILITY OF COLUMN AND PLATE STRUCTURES, Proceedings of the AIAA/ASME Eighth Structures, Structures Dynamics and Materials Conference, 1967, pp. 651-659.
23. Donnell, L. H., ON THE APPLICATION OF SOUTHWELL'S METHOD FOR THE ANALYSIS OF BUCKLING TEST, Timoshenko Anniversary Volume, Mc-Graw Hill Book Company, 1938, pp. 27-38.
24. Sabir, A. B., LARGE DEFLECTION AND BUCKLING BEHAVIOR OF A SPHERICAL SHELL WITH INWARD POINT LOAD AND UNIFORM PRESSURE, Journal of Mechanical Engineering Science, Vol. 6, No. 4, 1964, pp. 394-404.
25. Sendelbeck, R. L., THE MANUFACTURE OF THIN SHELLS BY ELECTROFORMING PROCESS, Stanford University Department of Aeronautics and Astronautics, SUDAER 185, April 1964, 20 pp.